

Key Points:

- Disentangle turbulence/cloud/precipitation processes over Amazon and reveal root cause for sensitivity to planetary boundary layer (PBL) schemes using the Weather Research and Forecasting model
- Free troposphere (FT) mixing becomes prominent in the presence of clouds, which in turn supports maintenance of the FT clouds that would otherwise dissipate
- Stronger vertical moisture relay transport in asymmetric convective model v2 (ACM2) PBL scheme supports thicker FT clouds, leading to reduced heating and precipitation

Supporting Information:

Supporting Information may be found in the online version of this article.

Correspondence to:

X.-M. Hu, M. Xue and H. M. Novoa,
xhu@ou.edu;
mxue@ou.edu;
hnovoa@unsa.edu.pe

Citation:

Hu, X.-M., Huang, Y., Xue, M., Martin, E., Hong, Y., Chen, M., et al. (2023). Effects of lower troposphere vertical mixing on simulated clouds and precipitation over the Amazon during the wet season. *Journal of Geophysical Research: Atmospheres*, 128, e2023JD038553. <https://doi.org/10.1029/2023JD038553>

Received 19 JAN 2023

Accepted 10 JUN 2023

Effects of Lower Troposphere Vertical Mixing on Simulated Clouds and Precipitation Over the Amazon During the Wet Season

Xiao-Ming Hu^{1,2} , Yongjie Huang¹ , Ming Xue^{1,2} , Elinor Martin² , Yang Hong³ , Mengye Chen³ , Hector Mayol Novoa⁴ , Renee McPherson⁵ , Andres Perez⁴ , Isaac Yanqui Morales⁴ , and Auria Julieta Flores Luna⁴ 

¹Center for Analysis and Prediction of Storms, University of Oklahoma, Norman, OK, USA, ²School of Meteorology, University of Oklahoma, Norman, OK, USA, ³School of Civil Engineering and Environmental Science, University of Oklahoma, Norman, OK, USA, ⁴Universidad Nacional de San Agustín de Arequipa, Arequipa, Peru, ⁵Department of Geography and Environmental Sustainability, University of Oklahoma, Norman, OK, USA

Abstract Planetary boundary layer (PBL) schemes parameterize unresolved turbulent mixing within the PBL and free troposphere (FT). Previous studies reported that precipitation simulation over the Amazon in South America is quite sensitive to PBL schemes and the exact relationship between the turbulent mixing and precipitation processes is, however, not disentangled. In this study, regional climate simulations over the Amazon in January–February 2019 are examined at process level to understand the precipitation sensitivity to PBL scheme. The focus is on two PBL schemes, the Yonsei University (YSU) scheme, and the asymmetric convective model v2 (ACM2) scheme, which show the largest difference in the simulated precipitation. During daytime, while the FT clouds simulated by YSU dissipate, clouds simulated by ACM2 maintain because of enhanced moisture supply due to the enhanced vertical moisture relay transport process: (a) vertical mixing within PBL transports surface moisture to the PBL top, and (b) FT mixing feeds the moisture into the FT cloud deck. Due to the thick cloud deck over Amazon simulated by ACM2, surface radiative heating is reduced and consequently the convective available potential energy is reduced. As a result, precipitation is weaker from ACM2. Two key parameters dictating the vertical mixing are identified, p , an exponent determining boundary layer mixing and λ , a scale dictating FT mixing. Sensitivity simulations with altered p , λ , and other treatments within YSU and ACM2 confirm the precipitation sensitivity. The FT mixing in the presence of clouds appears most critical to explain the sensitivity between YSU and ACM2.

Plain Language Summary Predictions of weather and climate in terms of clouds and precipitation over the Amazon in South America are quite uncertain. This uncertainty has been largely attributed to errors in the planetary boundary layer (PBL) scheme, which represents turbulent mixing. A lack of understanding of the relationship between turbulence, clouds, and precipitation processes prevents us from improving PBL representation in models to achieve better weather and climate simulations. This study disentangles the turbulence/clouds/precipitation relationship, and identifies the root cause of model errors in PBL schemes using regional climate simulations over the Amazon. Two PBL schemes, the Yonsei University (YSU) scheme, and the asymmetric convective model v2 (ACM2) scheme, are examined, which show the largest difference in the simulated precipitation. The main difference between the two PBL schemes is the dissipation (YSU) or maintenance (ACM2) of clouds during daytime above the boundary layer, which modulates surface heating and consequently precipitation. The maintenance of a thick cloud deck over the Amazon in ACM2, is caused by enhanced vertical transport of moisture from the surface to above the boundary layer. Such an improved understanding of the turbulence/clouds/precipitation relationship allow us to propose potential solutions to improve PBL schemes in weather and climate models.

1. Introduction

Climate change can cause shifted weather patterns, more extreme weather events, reduced water availability, change in agricultural patterns and increased exposure to disease (Langenbrunner et al., 2019; Prein et al., 2017; Vera, Silvestri, et al., 2006) and other significant impacts on society. Accurate simulation of regional climate and the development of adaptation strategies and corresponding policies are critical. Global climate model (GCM) simulations are too coarse to resolve local forcing and local weather, and their precipitation simulation is generally

poor. Cloud-resolving regional climate model (RCM) simulations have emerged in recent years for dynamically downscaling global climate simulations and climate change responses at spatial scales that are more useful for decision making (Y. Huang et al., 2023; C. Liu et al., 2022; Prein et al., 2015, 2017, 2022; Sun et al., 2016). However, compared to mid-latitude regions, the performance of RCM simulations in reproducing precipitation over tropical regions, such as the Amazon in South America, is understudied (Chakraborty et al., 2020; Prein et al., 2022; Tai et al., 2021).

Noontime and afternoon mesoscale convective systems (MCSs) are the main source of precipitation over the Amazon and thus Amazonian precipitation has a single afternoon peak in diurnal cycle (Giangrande et al., 2017, 2020; Prein et al., 2022; M. Wu et al., 2021). Moist advection from the Atlantic Ocean by northeasterly trade winds during the austral summer wet season (January–February) and zonal wind convergence are important for precipitation over the Amazon rainforest (Fu et al., 1999) and cloud and turbulence processes play critical roles in modulating precipitation in the region (Barber et al., 2022; Chakraborty et al., 2018; Chakraborty et al., 2020; Prein et al., 2022; Vilà-Guerau de Arellano et al., 2020; Wright et al., 2017). The relationship between processes of clouds, turbulence, and precipitation in the region remains to be disentangled and their modeling uncertainties and sensitivities need to be understood to improve simulations (Giangrande et al., 2017, 2020; Prein et al., 2022).

Simulated precipitation over the Amazon is sensitive to the planetary boundary layer (PBL) scheme, but the root cause for such sensitivity and the cause-effect relationship remain to be disentangled (Prein et al., 2022). Within typical weather and climate models, PBL schemes parameterize unresolved turbulent mixing within the PBL and the FT; the PBL schemes are therefore critical for reproducing the bulk boundary layer structures and profiles in the whole atmospheric column, as well as their subsequent effects on weather and climate simulations. Many studies (Gunwani & Mohan, 2017; Hu, Nielsen-Gammon, et al., 2010; Hu et al., 2012, 2019; Hu, Klein, & Xue, 2013; J. X. Wang & Hu, 2021) have evaluated the performance of various modern PBL schemes, with most of them focusing on continental cloud-free PBL. Compared to continental clear PBL, much less is known about the performance of PBL schemes in presence of clouds (Angevine et al., 2012; H. Y. Huang et al., 2013; Supinie et al., 2022; Valappil et al., 2023; Yang et al., 2019).

PBL schemes can be classified into local and nonlocal schemes. Local schemes estimate the turbulent fluxes at each point in a model from the mean atmospheric variables and/or their gradients at that point, whereas nonlocal schemes include turbulent fluxes based on the atmospheric variables and their variations over a deeper layer covering multiple model levels through the PBL (Cohen et al., 2015; Hu, Nielsen-Gammon, et al., 2010). The assumption among local schemes that fluxes depend solely on local values and local gradients of model state variables is least valid under convective conditions when turbulent fluxes are dominated by large eddies that transport fluid over longer distances (Hu, Nielsen-Gammon, et al., 2010). Previous studies found that traditional local schemes (e.g., Mellor–Yamada–Janjić (MYJ) or quasi-normal scale elimination (QNSE)) predict daytime continental boundary layers that are too cool and shallow; while schemes that include non-local treatment, such as the asymmetrical convective model, version 2 (ACM2, Pleim, 2007a), the Yonsei University (YSU, Hong et al., 2006) schemes and the more recently-updated local scheme (e.g., Mellor–Yamada Nakanishi and Niino (MYNN, Nakanishi & Niino, 2006)) predict deeper and warmer daytime continental boundary layers than MYJ and QNSE (Bright & Mullen, 2002; Clark et al., 2015; Coniglio et al., 2013). Also, nonlocal PBL schemes can reproduce the slightly stable upper convective boundary layer while local schemes often fail to do so (Hu et al., 2019; W. G. Wang et al., 2016).

Recent PBL development has started to use the mass flux (MF) approach that has been commonly used in cumulus parameterization schemes for large-eddy nonlocal mixing together with the eddy-diffusivity (ED) closure parameterizing local mixing, such as the MYNN-EDMF scheme (Angevine et al., 2010; Olson, Kenyon, Angevine, et al., 2019; Olson, Kenyon, Djalalova, et al., 2019; Pergaud et al., 2009). Note that MYNN-EDMF parameterizes specifically nonlocal mixing associated with shallow cumulus clouds, thus a convective parameterization is still needed to parameterize deep convection if the grid spacing is not fine enough to explicitly represent deep convection. Most previous PBL modeling studies focus on treatments within the boundary layer while free-troposphere treatments rarely receive much attention (Hu et al., 2012; Lu & Wang, 2019; Zhu et al., 2019, 2021), likely because that free-troposphere turbulence is weak under clear conditions and the impact of its parameterization on weather and climate simulations is regarded as minor.

Y. Huang et al. (2021, 2023) conducted nested-domain RCM simulations with grid spacings of 15 and 3 km over the Amazon with different physics schemes. It is found that the simulated precipitation is most sensitive to PBL schemes with the YSU scheme significantly overpredicting Amazonian precipitation and the ACM2

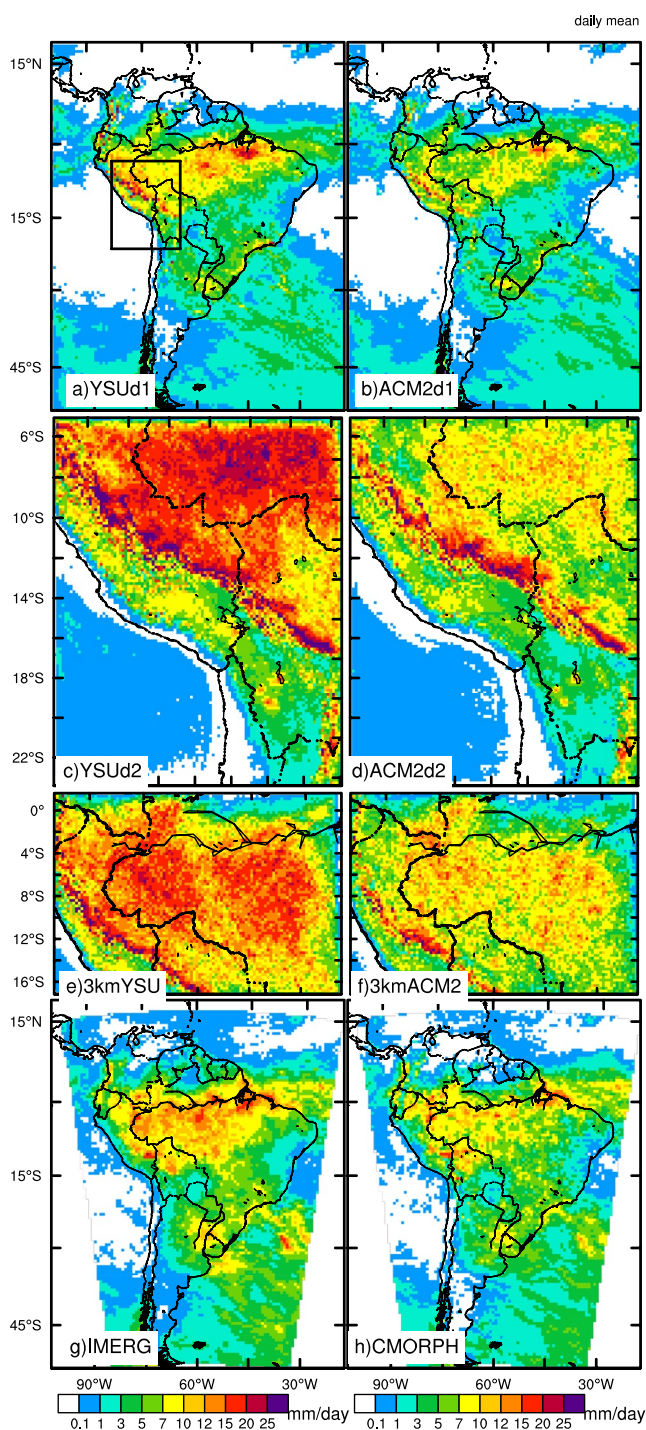


Figure 1. Daily mean precipitation rate in January–February 2019 simulated with (a) YSU in domain 1, (b) ACM2 in domain 1 with a 15 km grid spacing, (c) YSU in domain 2, (d) ACM2 in domain 2 with a 3 km grid spacing, (e) single-domain YSU, (f) single-domain ACM2 with a 3 km grid spacing and from (g) IMERG, (h) CMORPH data. The rectangle in (a) marks the location of the nested domain.

scheme predicting the weakest precipitation. Extending the work of Y. Huang et al. (2023), this study aims to understand the precipitation sensitivity over the Amazon at a process level and identify the root cause for the different model behaviors, with particular attention paid to the behaviors and effects of PBL schemes in cloudy environments, and both inside and above the PBL. Effects of lower troposphere vertical mixing on simulated clouds and precipitation over the Amazon will be elucidated.

The rest of this paper is organized as follows: In Section 2, precipitation data, model configurations, and numerical experiment design are described. In Section 3, clouds/precipitation sensitivity to PBL schemes is diagnosed using simulations with YSU and ACM2 and their variants with altered turbulence treatments, followed by discussion of such sensitivity at a finer resolution. Meanwhile the turbulence/cloud/precipitation processes over the Amazon are examined. Finally, Section 4 contains a summary and discussion of the main findings.

2. Precipitation Data, Model Configuration and Numerical Experiment Design

2.1. Precipitation Data

Two gridded global precipitation data sets are used in this study to compare with simulations, including (a) half-hourly Integrated Multi-satellE Retrievals for GPM (IMERG) at a horizontal resolution of $0.1^\circ \times 0.1^\circ$ (Huffman et al., 2019), and (b) half-hourly National Oceanic and Atmospheric Administration (NOAA) Climate Prediction Center (CPC) MORPHing Technique (CMORPH) global precipitation analyses at a horizontal resolution of ~ 8 km (Joyce et al., 2004).

2.2. Model Configurations

Y. Huang et al. (2021, 2023) used the Weather Research and Forecasting (WRF) model Version 4.2.1 (Skamarock et al., 2021; Skamarock & Klemp, 2008) to perform historical simulations over South America during January–February 2019 in preparation for future regional climate dynamic downscaling. The simulations used hourly European Centre for Medium-Range Weather Forecasts Reanalysis v5 (ERA5, Hersbach et al., 2020) for initial and boundary conditions. Two one-way nested domains with 15- and 3-km horizontal grid spacings cover the entire South America and the Peruvian central Andes region, respectively (see Figure 1a for domain coverage). Both domains use 61 stretched vertical levels topped at 20 hPa. Following previous dynamic downscaling practices (Hu et al., 2018; Miguez-Macho et al., 2004, 2005; J. L. Wang & Kotamarthi, 2013), spectral nudging technique is applied to the outer 15-km domain to maintain large-scale circulations at a 1,500 km scale, while allowing WRF to evolve smaller-scale dynamics and physics. Twelve sensitivity experiments were conducted by Y. Huang et al. (2023) with varied PBL, microphysics schemes, and land surface models (LSMs) while other physics parameterizations were kept the same among the sensitivity experiments, including revised MM5 Monin-Obukhov surface layer scheme (Jiménez et al., 2012), and the Rapid Radiative Transfer Model for GCMs (RRTMG) longwave and shortwave radiation scheme (Iacono et al., 2008).

Table 1

Model Configuration for Sensitivity Simulations Modifying Parameters and Treatments in the Yonsei University (YSU) and Asymmetric Convective Model v2 (ACM2) Planetary Boundary Layer (PBL) Schemes

PBL	Grid spacings (km)	Experiment name	Changed parameters/treatments
YSU	15	YSU	$p = 2$ (default)
		YSUp.5	$p = 0.5$
		YSUuseACM2free	Use free troposphere treatment from ACM2
		YSUp.5useACM2free	$p = 0.5$ & use free troposphere treatment from ACM2
	3	3kmYSU	$p = 2$ (default)
		3kmYSUp.5	$p = 0.5$
		3kmYSUp.5useACM2free	$p = 0.5$ & use free troposphere treatment from ACM2
		3kmACM2	$\lambda = 80$ (default)
ACM2	15	ACM2	$\lambda = 80$ (default)
	3	ACM2 $\lambda=30$	$\lambda = 30$
		3kmACM2	$\lambda = 80$ (default)

Note. p is an exponent in the polynomial function determining vertical mixing strength in the PBL, λ is the asymptotic length scale. The italic values are the adopted values in the sensitivity simulations.

The Tiedtke cumulus parameterization scheme (Tiedtke, 1989) is used on the 15-km outer domain to handle both shallow and deep convections but not on the 3-km inner domain.

These WRF downscaling simulations are found to be most sensitive to PBL schemes with the YSU scheme significantly overpredicting Amazonian precipitation, the ACM2 scheme predicting the weakest precipitation, and the MYNN-EDMF prediction being in the middle. Such relative differences are maintained with altered micro-physics schemes and LSMs. Simulations with the Thompson microphysics scheme (Thompson et al., 2008), and the Noah LSM (F. Chen & Zhang, 2009) are chosen to investigate PBL sensitivities in this study. Diagnosing the root cause for the differences between the YSU and ACM2 PBL schemes and disentangle the impact of PBL schemes on precipitation are the foci of this study. Since simulated precipitation is quite sensitive to some other parameterization, such as cumulus schemes (Hu et al., 2018), and there are large uncertainties among different precipitation data (M. Chen et al., 2022), recommending an optimal PBL scheme in terms of reproducing precipitation is beyond the scope of this study, which may require more advanced profile measurements (e.g., cloud water profile) and more accurate precipitation data to justify as will be seen in our later analyses.

2.3. Sensitivity Simulations With Altered Treatments in ACM2 and YSU

In addition to the simulations conducted by Y. Huang et al. (2023), eight more sensitivity simulations (summarized in Table 1) are run to help identify the root cause of the differences between ACM2 and YSU, and resolution dependence of the differences, as well as to examine impact of turbulent processes on cloud and precipitation processes. ACM2 and YSU differ in their treatments in both PBL and FT. Sensitivity simulations adjusting either PBL or free-troposphere mixing treatments or both are conducted.

In the PBL, while a counter-gradient term is added to the eddy diffusion equation to handle nonlocal mixing in YSU, ACM2 explicitly simulates the transient nonlocal MF. For the local mixing in the PBL, both ACM2 and YSU use a polynomial function/profile (so called K-profile, Noh et al., 2003) to define the vertical mixing coefficient K_z for temperature and moisture as:

$$K_z = Pr^{-1} k \frac{u_*}{\phi} z \left(1 - \frac{z}{h}\right)^p \quad (1)$$

where Pr is the Prandtl number, k is the von Karman constant, ϕ is the similarity profile function, z is the height above ground level, and h is the PBL height. Thus, ACM2 and YSU are also categorized into the K-profile PBL schemes (Hu et al., 2019). In YSU and ACM2, the value of the exponent p in Equation 1 is set to 2 by default, but its optimal value may vary from 0.5 to 3 depending on flow conditions, with a larger/smaller p yielding smaller/larger K_z (Hu, Zhang, et al., 2010; Hu et al., 2018; Nielsen-Gammon et al., 2010; Troen & Mahrt, 1986). While a similar local mixing treatment is adopted in ACM2 and YSU, there are many differences in their parameter

values, profile functions, methods to diagnose PBL height, etc. ACM2 generally simulates stronger vertical mixing in the PBL and higher PBL height under clear conditions (Hu, Nielsen-Gammon, et al., 2010). Since p effectively dictates the vertical mixing within the PBL, p is varied in sensitivity simulations to understand model differences and physics processes including turbulence, clouds, and precipitation (see experiment YSUP.5 in Table 1).

In the FT, only local mixing is considered in YSU and ACM2 (Hong, 2010; Nielsen-Gammon et al., 2010; Pleim, 2007b). Both YSU and ACM2 compute the K_z as a function of mixing length l , vertical wind shear S , and the stability function $f(Ri)$:

$$K_z = l^2 S f(Ri), \quad (2)$$

in which

$$\frac{1}{l} = \frac{1}{kz} + \frac{1}{\lambda}, \quad (3)$$

where Ri is the Richardson number, and λ is the asymptotic length scale. Such first-order parameterizations of turbulent vertical mixing are widely used in operational numerical weather prediction (NWP) and climate models (Beare et al., 2006; Cuxart et al., 2006). ACM2 and YSU differ in their parameter values, Ri calculation within clouds, and stability functions. Both ACM2 and YSU use moist-air Ri calculation adapted from Durran and Klemp (1982), but YSU requires two layers of clouds to activate the moist-air Ri calculation between the two layers while ACM2 only requires one layer, in addition to other differences in parameters. Note that these PBL parameterizations only consider local in-cloud turbulent mixing, non-local in-cloud mixing needs to be accounted for by a cumulus parameterization scheme on the convection-parameterized grid or explicitly resolved by the convection-permitting grid. Much of the improvement to such parameterizations (Equations 2 and 3) in NWP and climate models involved adjusting the stability functions (e.g., short vs. long-tailed functions) and λ (Cuxart et al., 2006). λ is adjustable and varies between 30 and 250 m in numerical models (Cuxart et al., 2006; M. Liu & Carroll, 1996; Nielsen-Gammon et al., 2010). λ is set to 30 m in the YSU scheme and to 80 m in the ACM2 scheme. Sensitivity simulations are conducted in this study by replacing the whole free-troposphere treatments (experiment YSUuseACM2free in Table 1) or only altering the value of λ (experiment ACM2λ30 in Table 1).

The sensitivity simulations are conducted with the outer 15 km domain because the difference between inner-domain outputs from our nested-domain runs with different configurations are rooted from the different simulations in the outer 15 km domain, as we will see in our analysis. Thus, the conclusions from these sensitivity simulations have implications for regional and global models that run at convection-parameterized resolutions. In addition, four sensitivity simulations with a single domain covering the majority of the Amazon with a 3 km grid spacing (experiments 3kmYSU, 3kmYSUP.5, 3kmYSUP.5useACM2free, 3kmACM2 in Table 1) are also conducted to examine the applicability of conclusions obtained at 15 km grid spacing to convection-allowing simulations.

3. Results

3.1. Cause of Precipitation Differences Simulated With Different PBL Schemes

As stated earlier, WRF simulations over South America during January–February 2019 are conducted with 12 different physics schemes, including PBL, microphysics schemes and LSMs (Y. Huang et al., 2023). The simulated precipitation is most sensitive to PBL schemes (Y. Huang et al., 2023) with the YSU scheme predicting the strongest daily precipitation rate while the ACM2 scheme predicting the weakest precipitation over the Amazon during the summer wet season (Figure 1). The relative strength of simulated precipitation between ACM2 and YSU remains across different resolutions, including the convection-parameterized (15 km grid spacing) and convection-permitting (3 km grid spacing) resolutions. The precipitation rate increases with increased resolution. The YSU runs at 3 km grid spacing (including the nested run focusing on Peru and the single-domain run focusing more on the Amazon) significantly overestimate daily precipitation rate (Figures 1c–1f). The South America Affinity Group (SAAG) led by National Center for Atmospheric Research (NCAR) also reported that a WRF simulation using the YSU scheme at a grid spacing of 4 km over South America overestimated precipitation over the Amazon (C. Liu et al., 2022).

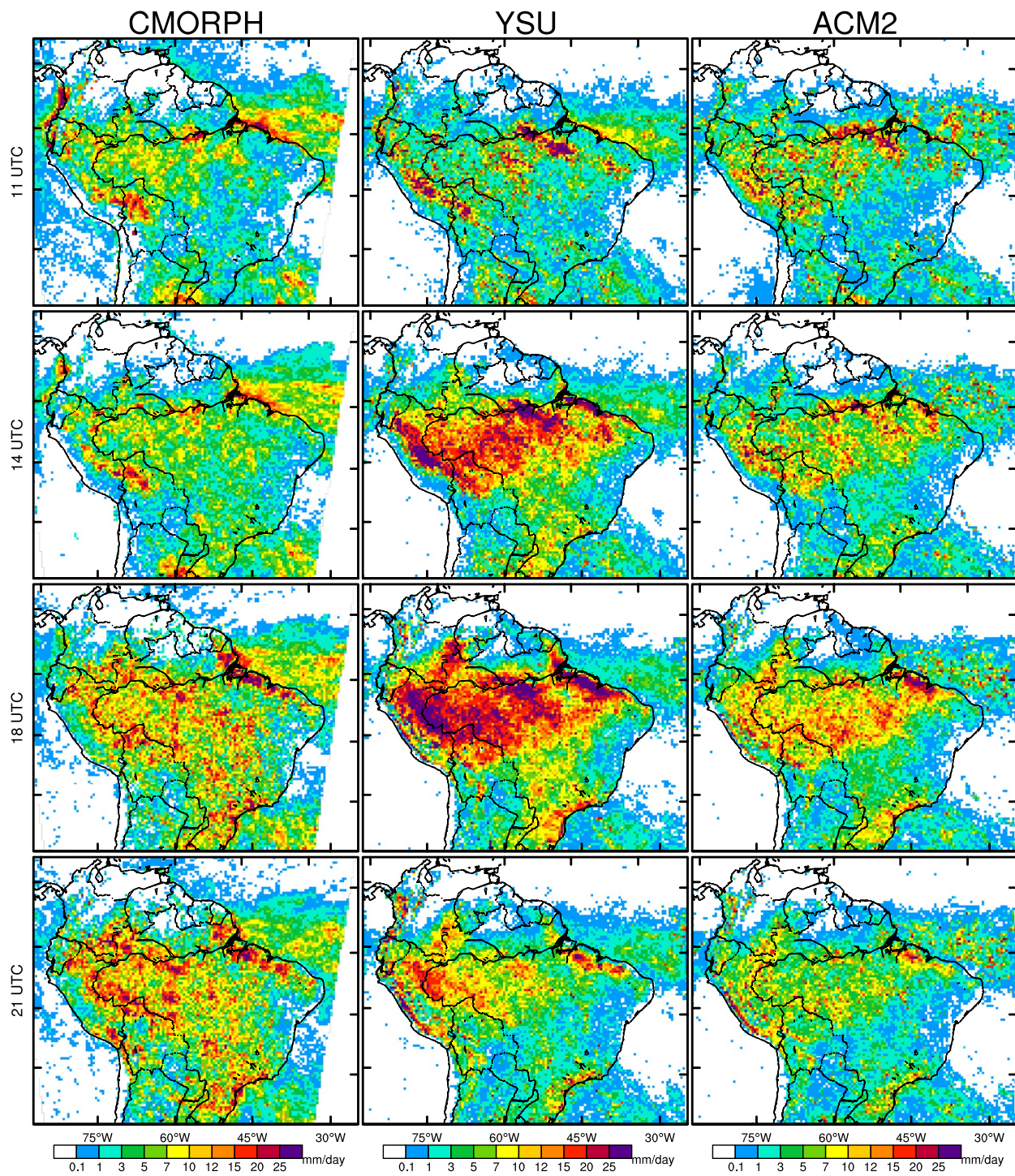


Figure 2. Mean precipitation rate over the Amazon in January–February 2019 from (left) CMORPH, and simulated by (middle) YSU and (right) ACM2 at (top to bottom) 11, 14, 18, and 21 UTC (7, 10, 14, 17 LST correspondingly).

Precipitation over the Amazon is dominated by mid-day and afternoon MCSs (Giangrande et al., 2017, 2020; Prein et al., 2022; M. Wu et al., 2021). Y. Huang et al. (2021, 2023) evaluated the simulated diurnal variation of precipitation. All WRF simulations with different configurations reproduce the afternoon precipitation peak with biases in intensity and timing. ACM2 scheme shows the best agreement with observations and the difference between different PBL schemes are most significant in the afternoon (Figure 2). Thus, we will focus on the precipitation and related processes during daytime. During mid-day hours, YSU simulates stronger hourly

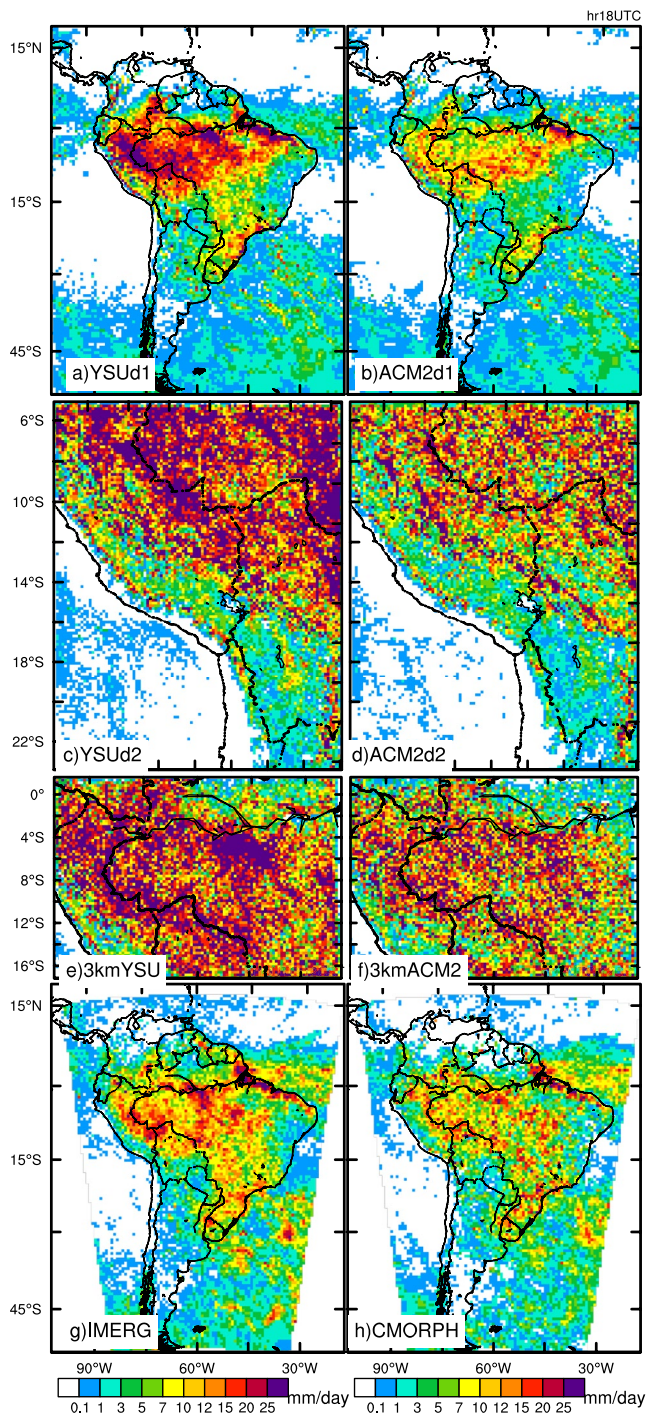


Figure 3. Hourly mean precipitation rate at 18 UTC (14 LST) in January–February 2019 simulated with (a) YSU in domain 1, (b) ACM2 in domain 1, (c) YSU in domain 2, (d) ACM2 in domain 2, (e) single-domain YSU, (f) single-domain ACM2 and observed from (g) IMERG, (h) CMORPH.

precipitation rates than ACM2 and overestimates precipitation at both resolutions and over different domains (Figures 2 and 3).

Causative factors for the different precipitation simulated by ACM2 and YSU over the Amazon are herein investigated. The impact of different PBL schemes on NWP and climate simulations is more straightforward under clear conditions while their impacts on precipitation is less clear. Often the impact of PBL schemes on precipitation is not conclusive because the schemes produce different (stronger or weaker) precipitation in different cases (Bright & Mullen, 2002; Cohen et al., 2015; Gopalakrishnan et al., 2023; Jankov et al., 2005, 2007; Li & Pu, 2008; Supinie et al., 2022; Z. Wu et al., 2021; Y. Zhang et al., 2013). Under clear conditions, ACM2 simulates stronger boundary layer vertical mixing and deeper PBL than YSU due to different treatments for nonlocal fluxes and different parameters/functions in the K -profile local mixing (Hu, Nielsen-Gammon, et al., 2010; Nielsen-Gammon et al., 2010; Shin & Hong, 2011; Xie et al., 2012). How such differences translate to significantly different precipitation with the two schemes is the main question to be answered in this study.

Surface temperature shows distinct differences over the Amazon with the ACM2 simulating lower continental temperatures than YSU by 0.5–0.8°C over the simulation domains around noon (Figure 4), which likely leads to less surface energy to feed MCSs. The lower temperature simulated by ACM2 covers the main precipitation region over the Amazon (Figure 4g) and can likely explain the precipitation difference. However, such temperature differences cannot be explained by the direct impact of PBL mixing. Prior work has shown that during daytime, ACM2 simulates stronger mixing in the PBL and stronger PBL-free troposphere exchange generally warming up the PBL due to entrainment of FT air with higher potential temperature (Hu, Nielsen-Gammon, et al., 2010; Shin & Hong, 2011). Thus, the direct impact of ACM2 PBL mixing should lead to higher surface temperature, rather than the lower temperature obtained in the regions of precipitation.

Rather, the temperature difference between ACM2 and YSU simulations is more directly related to the difference in surface downward shortwave radiation. ACM2 simulates less shortwave radiation at the surface over the Amazon region (Figure 5g), where cloud coverage is significant (Figure 5j). At 17 UTC (12–14 LST across south America), the average surface shortwave radiation simulated by ACM2 is lower by ~70 W m⁻² than the YSU runs. Thus, the lower temperature simulated by ACM2 should be due to indirect effects of vertical mixing via interactions with clouds and radiation.

Significant cloud coverage over the Amazon (Kay et al., 2012, 2016) is a characteristic distinguishing this study from most other studies of PBL schemes. Over the Amazonian region, ACM2 simulates a thicker cloud deck (Figures 6 and 7), which reduces downward shortwave radiation (Figure 8), consequently leading to a lower surface temperature. As a result, the surface-based convective available potential energy (CAPE) is lower in the ACM2 simulations (Figure 9), which would lead to weaker daytime precipitation. The significant difference between YSU and ACM2 is mostly confined over the cloud region (Figures 5 and 8), which further confirms that indirect effects of vertical mixing over the Amazon via interactions with clouds dominate its direct effects.

The cloud deck over the Amazon therefore appears to be a critical link to disentangle the impact of PBL schemes on simulated precipitation. The low-level clouds are produced by shallow convections and mid-level clouds are produced by deep convections either from isolated convective towers typically in daytime or from propagating MCSs typically during nighttime. During daytime, while the clouds simulated with the YSU scheme

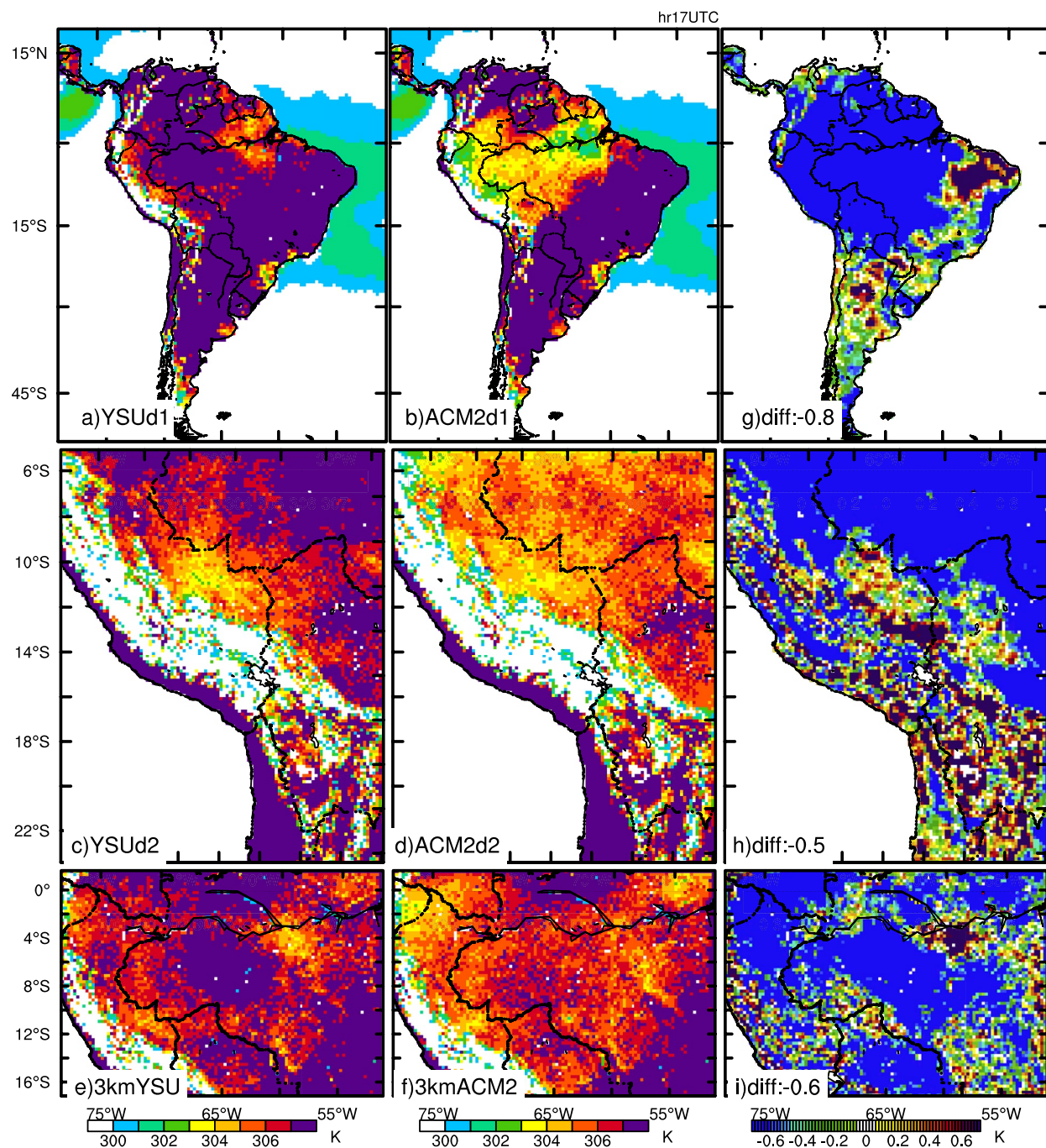


Figure 4. Average surface temperature at 17 UTC in January–February 2019 from (a, c, e) YSU, (b, d, f) ACM2, and (g, h, i) their difference (ACM2-YSU) in (top to bottom) different domains. The average difference over land is marked at the lower-left corner in (g, h, i).

dissipate gradually from the early morning maxima, clouds simulated with the ACM2 scheme are still sustained through the day (see cloud cross-sections at 11–21 UTC in Figure 6). Daytime cloud thinning is likely due to solar heating under condition of lack of water vapor supply available for condensation (Adebiyi et al., 2020; Burleyson & Yuter, 2015; Painemal et al., 2015; D. Zhang et al., 2010). The thicker cloud deck simulated by ACM2 appears to be due to enhanced supply of boundary layer moisture to the layers above (Figure 10a), thus less boundary layer moisture by 0.6 g kg^{-1} and more FT moisture by 0.2 g kg^{-1} compared to the YSU run (Figure 10b), through enhanced boundary layer vertical mixing (Hu, Nielsen-Gammon, et al., 2010; Shin & Hong, 2011).

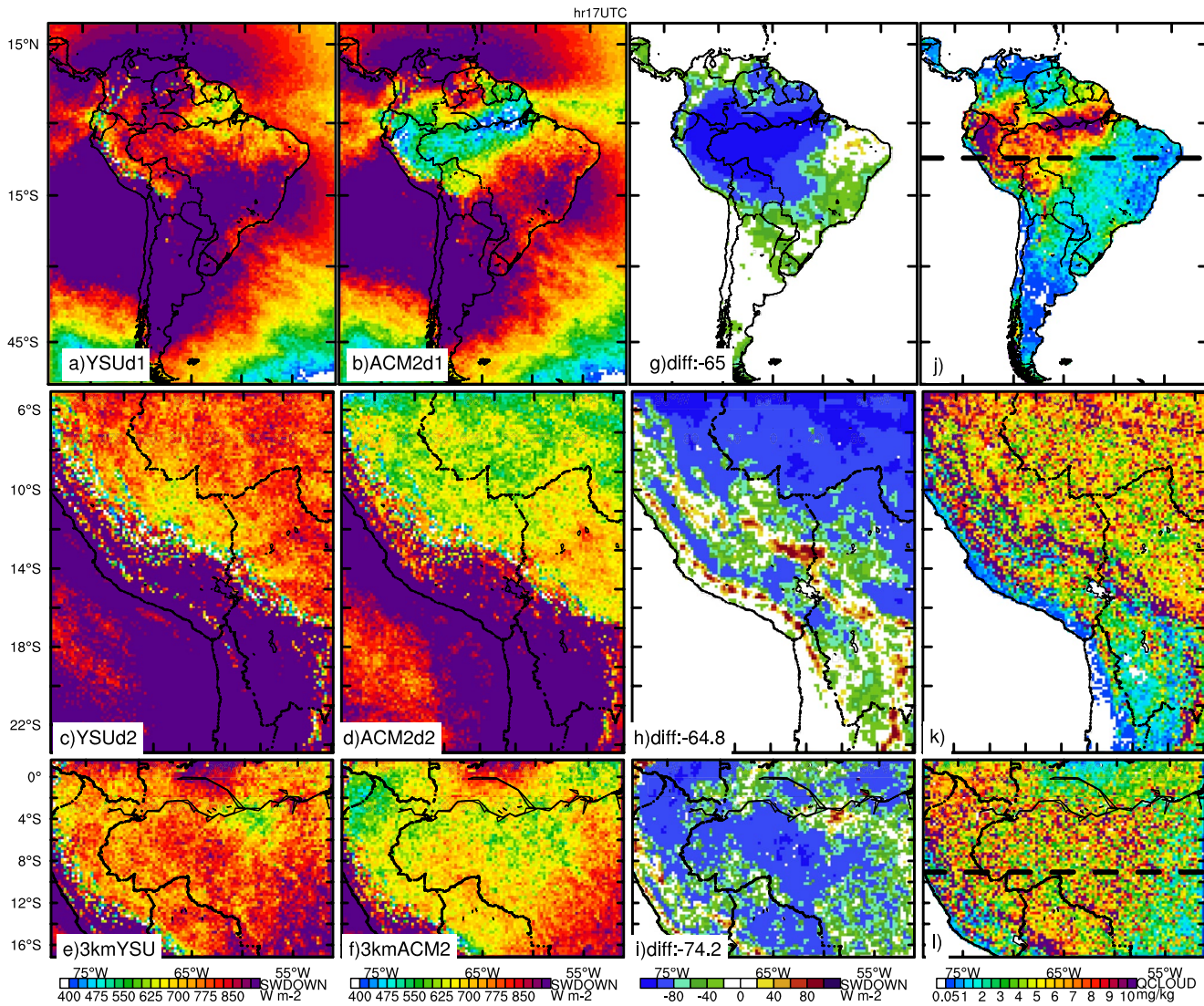


Figure 5. Average surface downward shortwave radiation at 17 UTC in January–February 2019 simulated with (a, c, e) YSU, (b, d, f) ACM2, (g, h, i) their difference, and (j, k, l) column-average cloud water mixing ratios in (top to bottom) different domains. The straight dash lines mark the location of cross-sections in Figures 6, 7, and 12.

In the nested-domain simulations, surface temperature simulated by ACM2 is lower than YSU in both 15 and 3 km domains (Figure 4) and the resulting lower precipitation occurs in both domains. The root cause of lower surface temperatures from ACM2 in the nested 3 km domain is less clear due to the possible effect of 15 km simulations via advection through its lateral boundaries. Thus, the main discussions below (in Section 3.2) will focus on further investigation of PBL-clouds-precipitation relationship in the outer 15 km domain with additional simulations with altered treatments, while their relationship at the convection-permitting resolution will be examined with additional single-domain simulations with a 3 km grid spacing (in Section 3.3).

3.2. Impact of Different Turbulence Treatments on Clouds and Precipitation

Lower troposphere turbulence plays important roles in cloud production and maintenance (Lilly, 1968). This section discusses results of sensitivity simulations adjusting turbulence treatments in YSU and ACM2. Since under clear conditions, ACM2 has stronger daytime boundary layer mixing than YSU (Hu, Nielsen-Gammon, et al., 2010; Shin & Hong, 2011), vertical mixing in the YSU PBL scheme is first enhanced to see if the simulated clouds and precipitation would become closer to those simulated by ACM2. The exponent p in the K -profile in

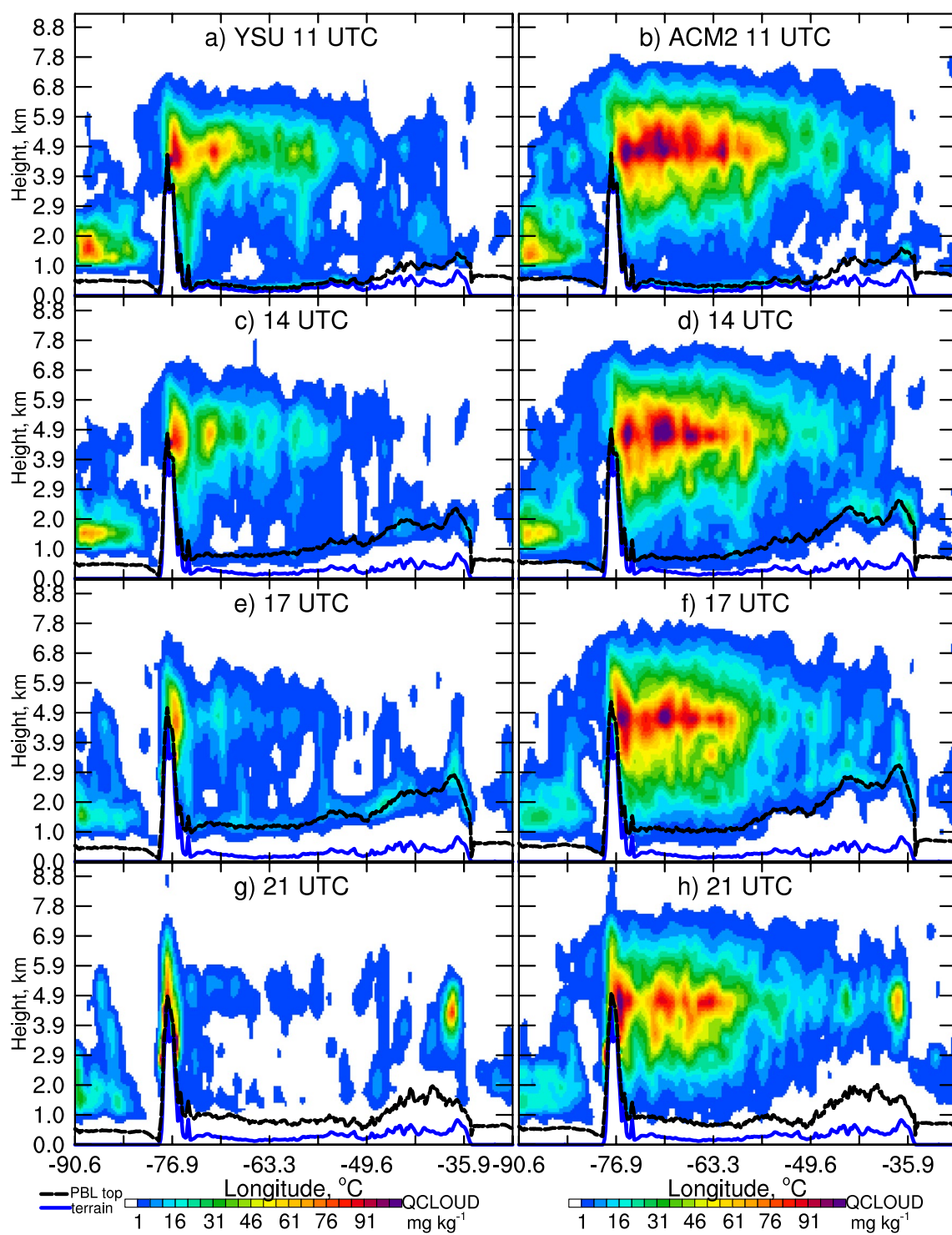


Figure 6. Averaged cross-section of cloud water over the Amazon of each day in January–February 2019 simulated by (left) YSU and (right) ACM2 at (a, b) 11, (c, d) 14, (e, f) 17, and (g, h) 21 UTC (7, 10, 13, 17 LST correspondingly). The location of these cross-sections is marked in Figure 5j. The dashed black line and continuous blue line indicate planetary boundary layer (PBL) top and terrain surface.

YSU (default value is 2) is reduced to 0.5 in experiment YSUp.5 to enhance daytime boundary layer mixing, as indicated by the K_z profiles in Figure 10d. With $p = 0.5$, YSUp.5 simulates higher PBL top height (Figure 10d). As a result, more near-surface moisture is transported to the top of the elevated PBL, where a thicker cloud layer near the PBL top forms (Figures 7c and 10c). Note that while the nonlocal mixing is proportional to K_z in

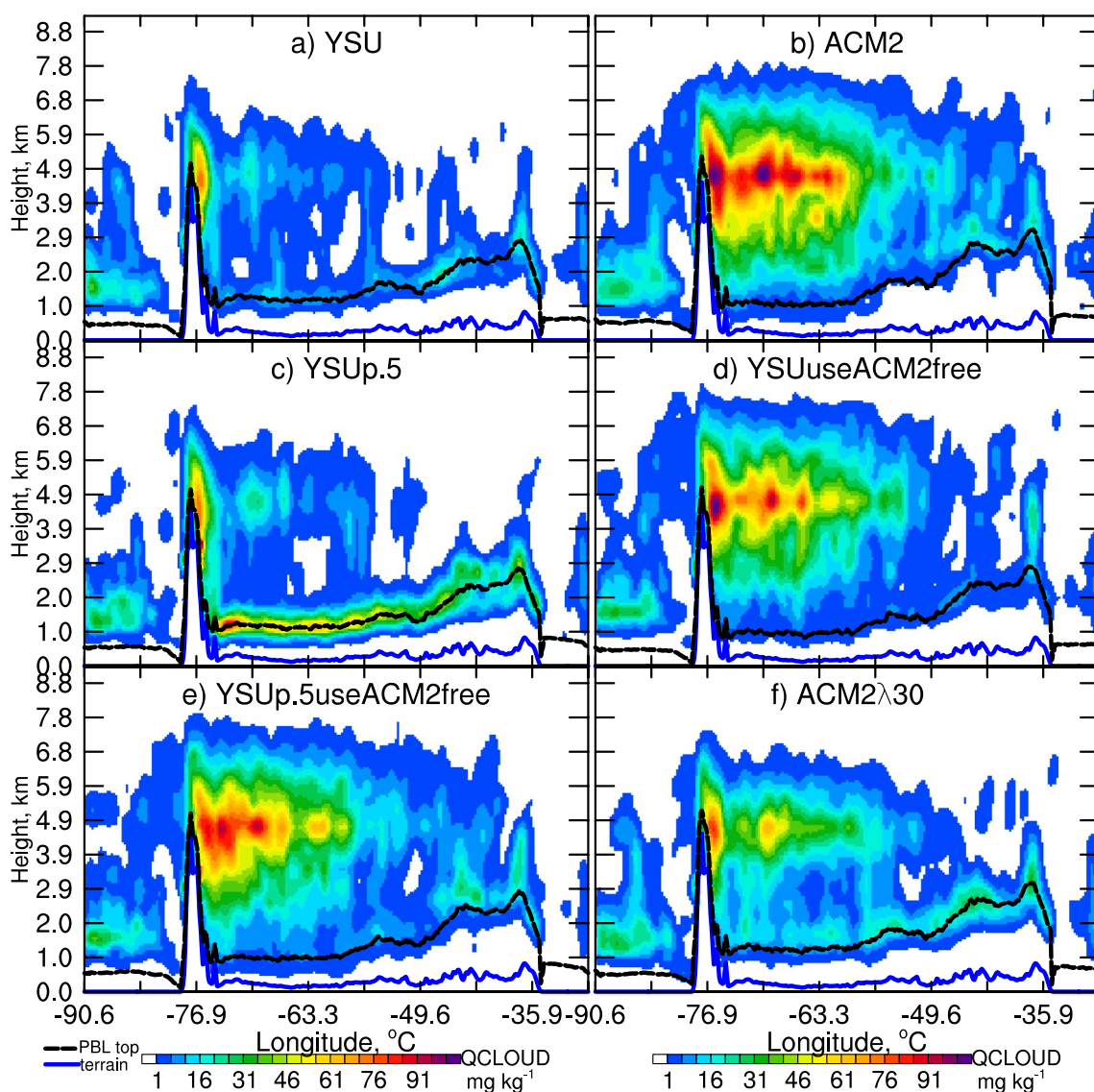


Figure 7. Cross-section of cloud water over the Amazon in January–February 2019 simulated by (a) YSU and (b) ACM2, (c) YSUP.5, (d) YSUuseACM2free, (e) YSUP.5useACM2free, (f) ACM2 λ 30 at 17 UTC. The location of these cross-sections is marked in Figure 5j.

YSU, transients nonlocal fluxes are explicitly simulated by ACM2, which is not shown in Figure 10. Thus K_z profiles in Figure 10d are more indicative of total mixing in the boundary layer for YSU, but less so for ACM2. In the FT where there are no nonlocal mixing treatments for either scheme, thus K_z profiles are indicative of free-troposphere mixing for both.

As the PBL grows in the daytime, the PBL top clouds simulated by both YSU and ACM2 keep elevating (Figure 6). A more prominent/distinct PBL top cloud layer is simulated by YSU (Figures 6c and 6e, PBL top is marked by black dash lines) while the PBL top clouds simulated by ACM2 are indistinctive from the free-troposphere clouds (Figures 6d and 6f). Existence of a PBL top cloud layer over the Amazon was previously illustrated by cloud frequency data observed during the GoAmazon 2014/5 field experiments (Giangrande et al., 2017, 2020). However, that data set only provides cloud frequency, not cloud amount. To quantitatively verify the simulated PBL top cloud layer, more advanced cloud data set is needed.

The thickened PBL top clouds simulated by YSU with $p = 0.5$ weakens surface shortwave radiation (Figure 8) and consequently lowers surface temperature and CAPE (Figure 9), thus reduces precipitation (Figure 11). Such a precipitation sensitivity to boundary layer mixing over the Amazon is consistent with that reported over the

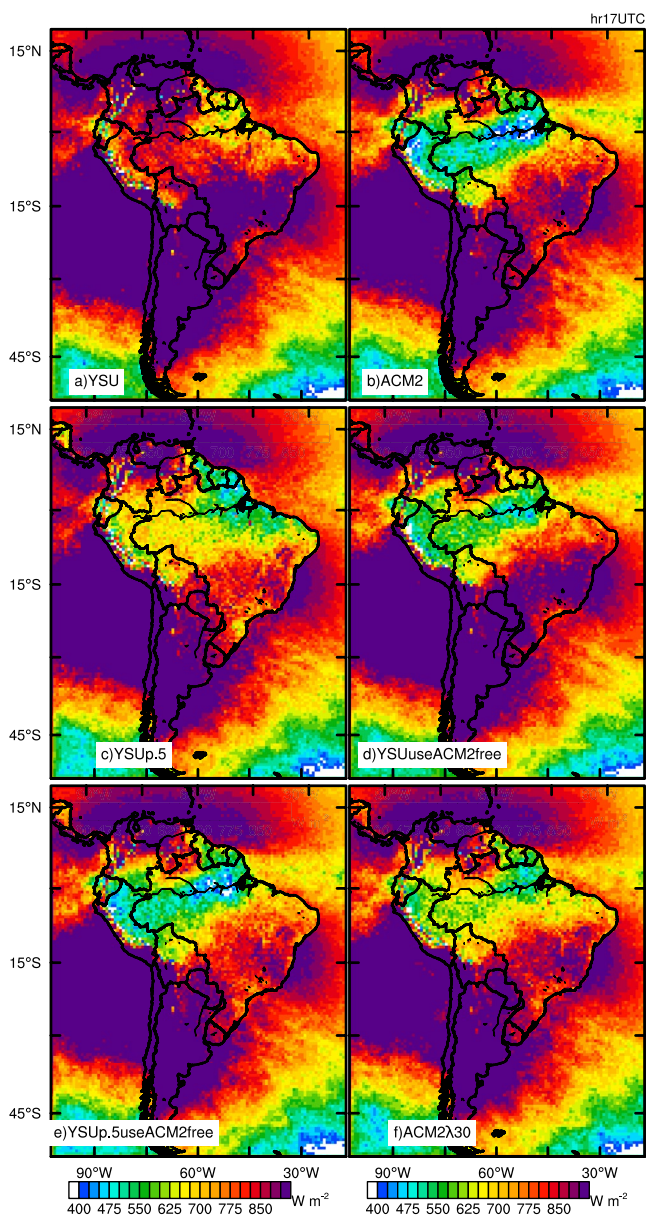


Figure 8. Average surface downward shortwave radiation at 17 UTC during January–February 2019 simulated by (a) YSU, (b) ACM2 and four sensitivity simulations (c) YSUp.5, (d) YSUuseACM2free, (e) YSUp.5useACM2free, (f) ACM2 λ 30.

(Figure 10d), and consequently a much thinner cloud deck at 4–5 km above ground and meanwhile the PBL top clouds appear thicker (Figure 7f), due to weaker vertical transport of moisture from the PBL top to higher levels (Figure 10a). The net result is that the surface radiation is enhanced (Figure 8f), temperature is higher, and more precipitation is produced (Figure 11f). The precipitation simulated by ACM2 λ 30 is not as strong as that simulated by YSU because of other differences in free-troposphere and PBL mixing treatments.

All the above results together suggest a prominent *PBL-free-troposphere moisture relay transport process*: Step 1, boundary layer mixing transports moisture to the PBL top where clouds form; step 2, free-troposphere mixing transports the moisture further to higher levels (~4–5 km) to sustain a thick cloud deck at that altitude and reduce the boundary layer top clouds somewhat. *ACM2 simulates a strong PBL-free-troposphere moisture relay transport process*. Comparing to YSU, ACM2 simulates less PBL moisture (by 0.5 g kg⁻¹) and

eastern United States (Hu et al., 2018). However, YSU with $p = 0.5$ does not reduce precipitation to the level simulated by ACM2 (Figure 11). In comparison, ACM2 simulates a more prominent cloud layer at a higher elevation (~4–5 km above ground) while the clouds simulated by YSU at this altitude (with both default p value and $p = 0.5$) weaken in time during the day (Figure 6). Thus, boundary layer mixing alone cannot completely explain the different impacts of ACM2 and YSU on clouds.

In addition to the different treatments within the boundary layer, ACM2 and YSU also differ in their treatments in the FT. A YSU sensitivity simulation using ACM2's free-troposphere mixing treatment (named YSUuseACM2free) is conducted to examine the impact of FT mixing. YSUuseACM2free simulates a stronger vertical mixing up to 7–8 km above the ground, particularly in the presence of clouds, similar to the ACM2 simulation (Figure 10d). In the absence of clouds, the free-troposphere mixing simulated by different PBL schemes are all similar and weak (Figure S1 in Supporting Information S1). Higher aloft (>8 km), ice and snow clouds dominate and peak in the afternoon (likely due to detrainment of deep convection), and the sensitivity of vertical mixing is small and K_z is simulated to be mostly less than 1 m² s⁻¹ by all schemes. Thus, our analysis focuses on the lower FT. As a result of stronger mixing in the lower FT, a thicker cloud deck at 4–5 km above ground (Figure 7d), similar to ACM2 (Figure 7b), develops in the simulation, due to stronger moisture supply from the PBL top (Figure 10a). Consequently, surface temperature is reduced due to cloud shield, and the precipitation is reduced, to be closer to that of ACM2 than YSUp.5 (Figure 11). Combining both $p = 0.5$ and ACM2's free-troposphere mixing, YSUp.5useACM2free simulates a similar, but slightly thicker cloud deck (Figure 7e) and slightly weaker precipitation than YSUuseACM2free (Figure 11). The mean free-troposphere clouds over Manaus (Figure 10c) simulated by YSU, YSUp.5, YSUuseACM2free, YSUp.5useACM2free, ACM2 are 15.4, 17.5, 62.6, 73.7, 72.4 mg kg⁻¹ respectively, among which the ones using ACM2's free-troposphere treatment are grouped together. Different clouds are the net results of the different K_z , which is as large as a factor of >20 in the FT in the presence of clouds. These experiments illustrate that free-troposphere mixing is the most critical difference between YSU and ACM2 in terms of simulating clouds and precipitation, while the mixing in the PBL plays a secondary role.

For FT vertical mixing, ACM2 and YSU differ in their parameters, moist-air Ri calculation, and the stability functions. Previous studies identified λ as a critical parameter for free-troposphere mixing (Cuxart et al., 2006; Hu et al., 2012; Nielsen-Gammon et al., 2010), and here its impact is further examined. An ACM2 sensitivity simulation with $\lambda = 30$ (named ACM2 λ 30) is conducted to verify its impact on clouds/precipitation. Comparing to default ACM2 with $\lambda = 80$, ACM2 λ 30 simulates a much weaker mixing in the FT

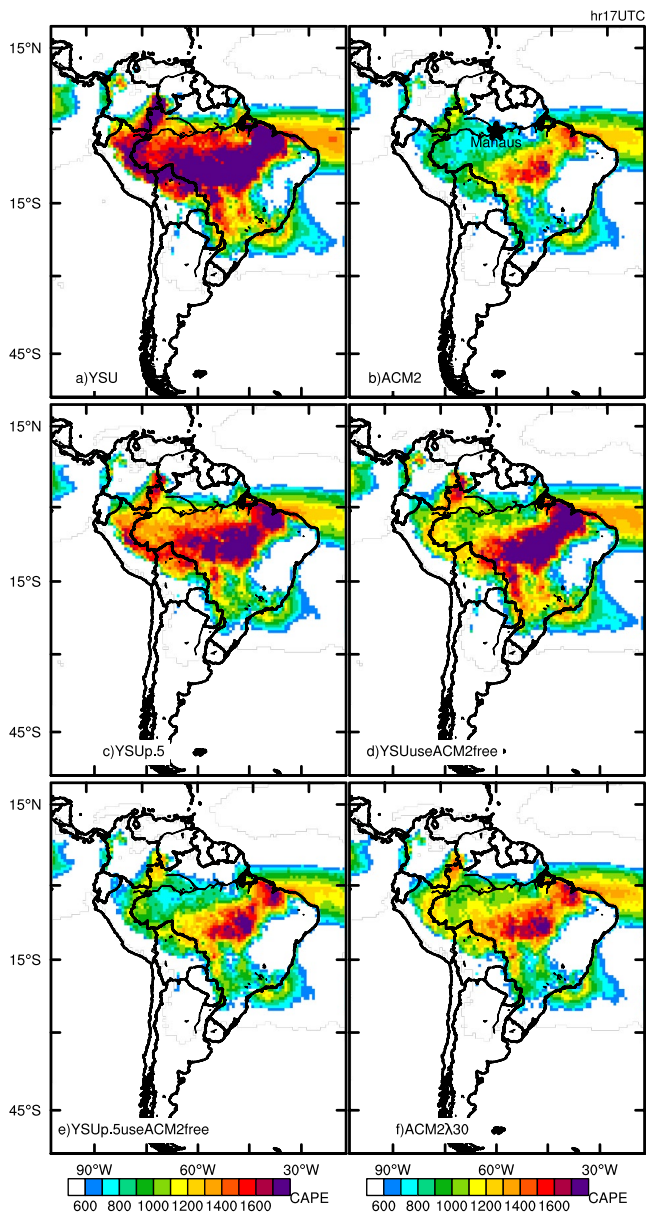


Figure 9. Average convective available potential energy at 17 UTC during January–February 2019 simulated by (a) YSU, (b) ACM2 and four sensitivity simulations (c) YSUp.5, (d) YSUuseACM2free, (e) YSUp.5useACM2free, (f) ACM2λ30.

more FT moisture (by 0.2 g kg^{-1} at 3–6.5 km above ground, Figure 10b) in monthly average. Consequently, the free-troposphere cloud layer is better maintained during daytime. In contrast, the moisture relay transport process simulated by YSU is weaker and the clouds at $\sim 4\text{--}5$ km dissipate quicker during daytime, leading to less cloud coverage, more CAPE and precipitation. Modified YSU with enhanced PBL and free-troposphere mixing (YSUp.5useACM2free) produces similar moisture transport as ACM2 (Figures 10b and 10d) hence reduced precipitation. These results suggest that free-troposphere mixing may become prominent in the presence of clouds (which otherwise would be weak as generally regarded) and become an important step in the relay transport process. To verify the strength of such relay transport process, more advanced observations, such as long-term vertical profiles of cloud mixing ratios, are warranted. Our results also suggest that to correctly simulate clouds/precipitation in environments similar to those of the Amazon, the ability of models in reproducing such moisture relay transport processes needs to be carefully assessed.

3.3. Sensitivity of Clouds and Precipitation to Different Turbulence Treatments at a Convection-Allowing Resolution

The sensitivity of simulated clouds and precipitation to boundary layer and free-atmosphere vertical mixing discussed above is mainly based on simulations at 15 km grid spacing where cumulus parameterization is employed. Thus, the conclusions are directly applicable to global and regional weather and climate simulations/predictions at convection-parameterized resolutions. Whether these conclusions are still valid at convection-permitting resolutions requires additional examination. To avoid the possible effects of the driving 15 km grid on the nested 3 km grid, single-domain sensitivity simulations are conducted that cover a majority of the Amazon with a 3 km grid spacing that use ERA5 data directly as lateral boundary conditions. These simulations include 3kmYSU, 3kmYSUp.5, 3kmYSUp.5useACM2free, and 3kmACM2 (as summarized in Table 1). Even though simulated precipitation rate is generally higher at the 3 km grid spacing than at 15 km grid spacing, the same turbulent mixing → clouds → precipitation impact/sensitivity holds in these convection-permitting simulations (Figures 12 and 13). That is, (a) YSU simulates stronger daytime precipitation rate than ACM2 (by 60% at noon time, 16 vs. 10 mm day^{-1} , Figures 13a and 13b); (b) Stronger boundary layer mixing simulated by YSU with $p = 0.5$ leads to more PBL top clouds (Figure 12c), which block more shortwave radiation and reduce daytime surface temperature and consequently precipitation (with 13 mm day^{-1} at noon, Figure 13c); (c) Using the free-troposphere mixing treatment of ACM2 in YSU simulates a more prominent cloud layer at 4–5 km above ground (Figure 12d) which more effectively blocks shortwave radiation and reduces precipitation (with 11 mm day^{-1} at noon, Figure 13d) that is closer to the precipitation rate of ACM2 (Figure 13b).

We repeated our simulations with the scale-aware Grell-Freitas scheme turned on over both 15-km and 3-km domains. The total simulated precipitation is enhanced compared with that using the Tiedtke cumulus scheme (Figures S2–S5 in Supporting Information S1), which is consistent with our previous study over the southern Great Plains (Hu et al., 2018). The sensitivity of simulated precipitation/clouds to different PBL schemes/treatments (the main focus of this study), however, remains the same (Figures S2–S5 in Supporting Information S1).

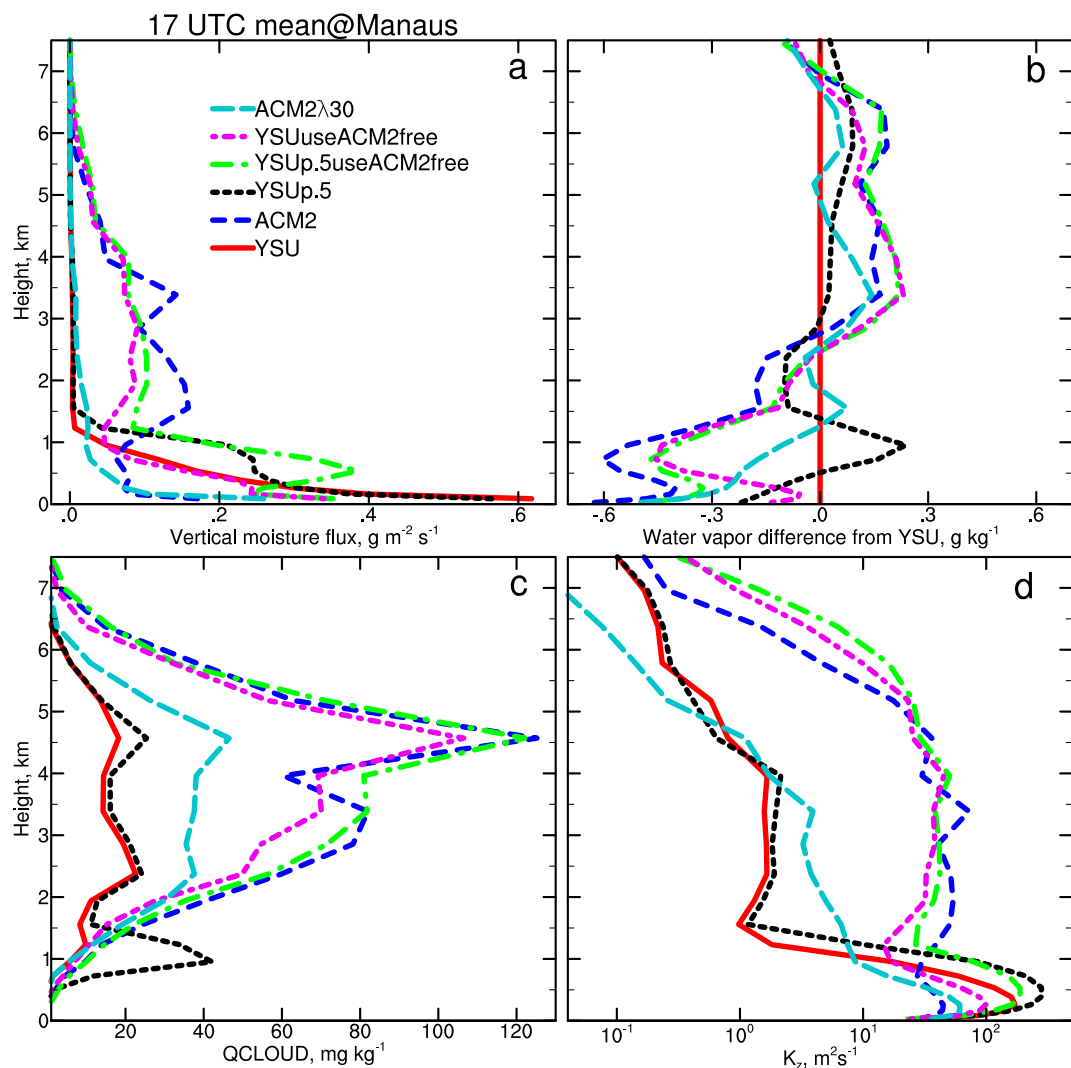


Figure 10. Mean profiles of (a) vertical moisture flux, (b) water vapor difference from that simulated by YSU, (c) cloud water mixing ratio (QCLOUD), and (d) vertical mixing coefficient (K_z) at 17 UTC during January–February 2019 at Manaus (location marked in Figure 9b) simulated by YSU, ACM2 and four sensitivity simulations YSup.5, YSUuseACM2free, YSup.5useACM2free, ACM2λ30.

4. Conclusions and Discussion

Previous studies by others and a recent study of ours found that precipitation simulations over the Amazon in South America are very sensitive to the PBL scheme used. The exact relationship between the turbulent mixing and precipitation processes in that humid region is, however, not clear. In this study, two-month-long simulations over South America in January–February 2019 are examined to understand the precipitation sensitivity to treatments of turbulent mixing in both the PBL and FT within PBL schemes. Two PBL schemes, the YSU and ACM2 schemes, are the foci of this study since they produced the most and least amount of precipitation among PBL schemes examined. Our results serve to disentangle the turbulence–cloud–precipitation processes over the Amazon and reveal root causes for the sensitivity to PBL schemes, which is a prerequisite for future model improvement. During daytime, while the free-troposphere clouds simulated by YSU dissipate due to solar heating, clouds simulated by ACM2 maintains through the day because of enhanced moisture supply due to enhanced *PBL-free-troposphere* relay transport process: step 1, enhanced vertical mixing within PBL simulated by ACM2 transports surface moisture to the PBL top where clouds first form, and step 2, enhanced free-troposphere mixing feeds the moisture into the free-troposphere cloud deck. Due to the thicker cloud deck over the Amazon simulated by ACM2, surface radiative heating is reduced and consequently CAPE

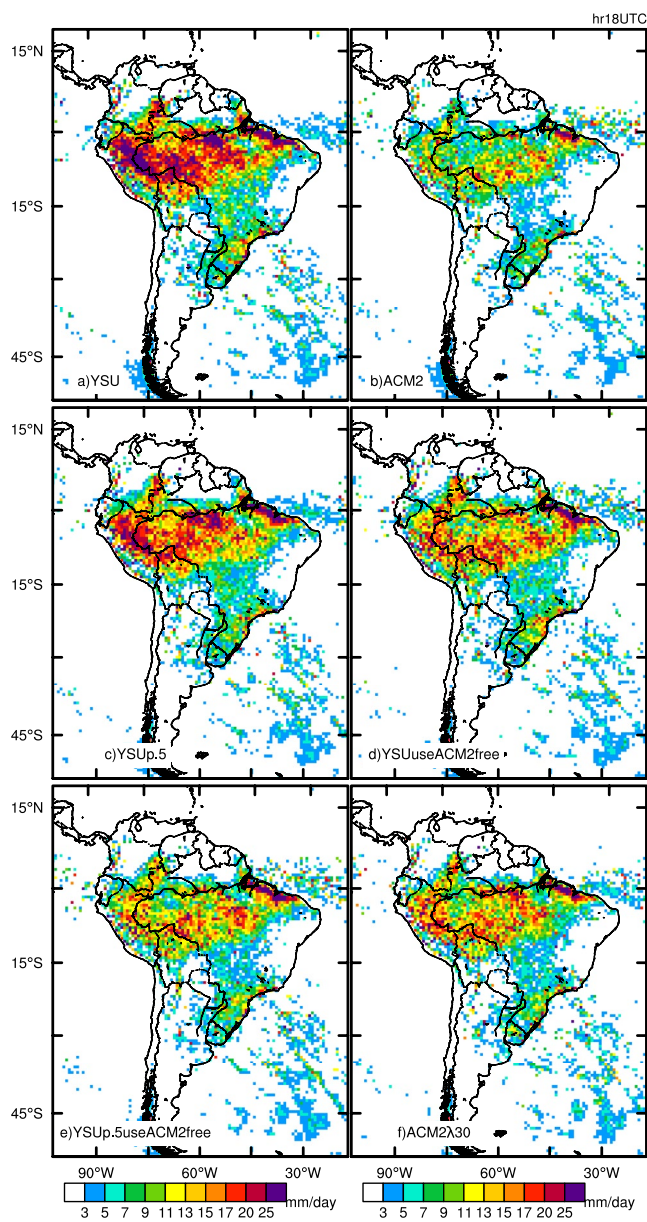


Figure 11. Average precipitation rate at 18 UTC during January–February 2019 simulated by (a) YSU, (b) ACM2 and four sensitivity simulations (c) YSUP.5, (d) YSUP.5useACM2free, (e) YSUP.5useACM2free, (f) ACM2 λ 30.

is reduced. As a result, precipitation is weaker from ACM2. In contrast, the moisture *PBL-free-troposphere* relay transport process simulated by YSU is weaker and the clouds at \sim 4–5 km dissipate quicker, and CAPE is therefore larger during daytime, leading to more precipitation. To verify the strength of such relay transport process, more advanced observations are warranted, for example, of long-term vertical profiles of cloud mixing ratios. To correctly simulate clouds and precipitation, model performance of reproducing such a moisture relay transport process needs to be carefully evaluated.

Two key parameters dictating the vertical mixing in the YSU and ACM2 schemes are identified, which are p , an exponent in the polynomial function determining boundary layer vertical mixing and λ , the asymptotic length scale dictating free-troposphere mixing. Sensitivity simulations with altered p , λ , and other treatments within YSU and ACM2 confirm the sensitivity of precipitation to the mixing strength. Calibrating parameters (p , λ) in YSU and ACM2 or improving their parameterization with non-constant values may be needed for general improvement to simulation results, although this is beyond the scope of this study.

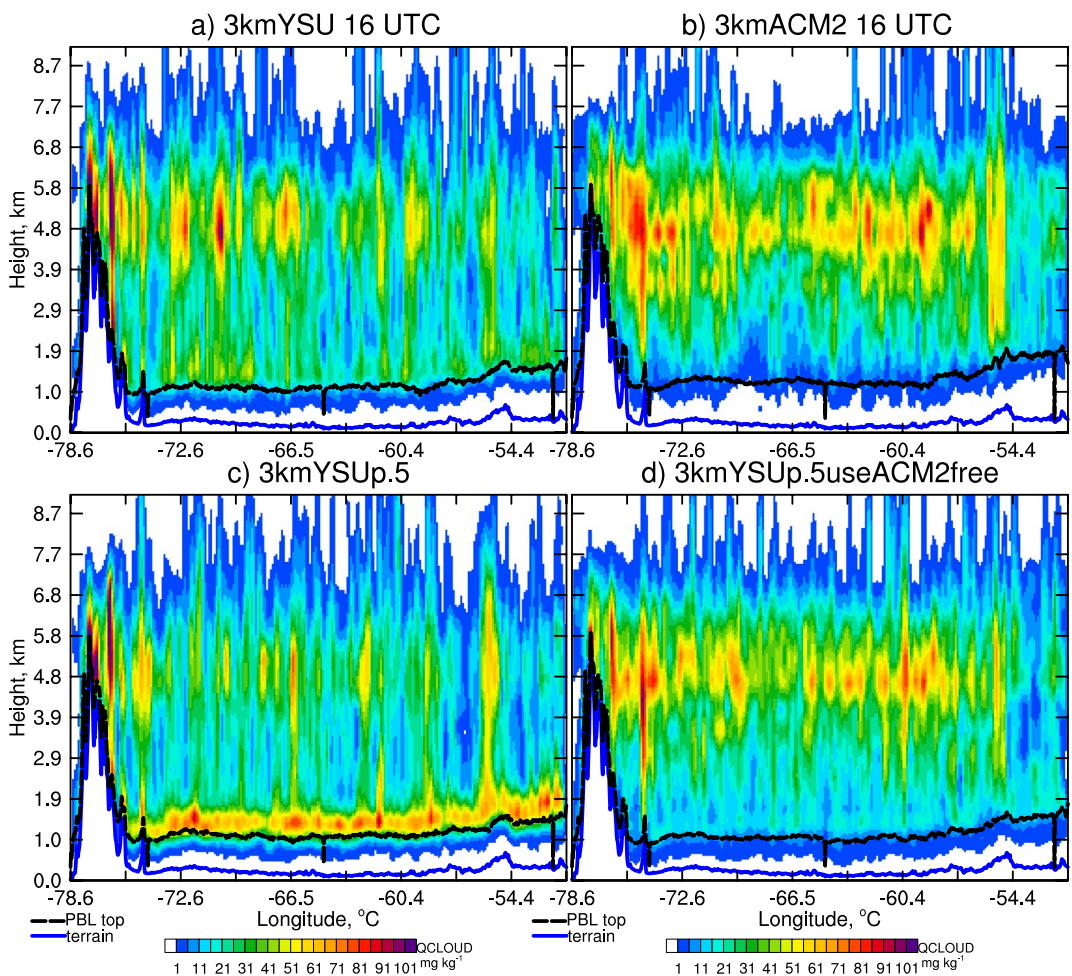


Figure 12. Cross-section of average noon-time cloud water mixing ratios over the Amazon in January–February 2019 simulated by (a) 3kmYSU, (b) 3kmACM2, (c) 3kmYSUp.5, and (d) 3kmYSUp.5useACM2free. The location of these cross-sections is marked in Figure 5*I*.

The free-troposphere mixing in presence of clouds become prominent (which is otherwise weak) because of reduced moist static stability and the difference in free-troposphere mixing appears to explain more of the sensitivity to the YSU and ACM2 PBL schemes. The turbulent mixing and cloud relationship over the Amazon simulated with ACM2 suggests strong positive feedback through which regions of lower troposphere clouds create conditions favorable for daytime cloud maintenance. Such feedback is weaker with YSU, which leads to daytime breakup of free-troposphere clouds.

The above results regarding the turbulence-clouds-precipitation processes and their parameterizations have important implications to the understanding and accurate prediction of weather, climate, as well as air quality over the Amazon region that is humid, cloudy and rich in precipitation. South America is experiencing an increasing trend in summer precipitation (Adler et al., 2017), and such a trend is also projected by some climate models (Vera, Silvestri, et al., 2006). Given the negative cloud-precipitation correlation seen in this study for the Amazon region, such a precipitation trend may imply a decreasing trend of cloud cover in the region. Correct representation of turbulence mixing-cloud-radiation interactions within weather and climate models is clearly critical for accurate simulation/prediction of precipitation and water cycles.

Though not shown here, the precipitation over Amazon appears to affect the strength of the south American LLJ. The convection over the Amazon produces upward motion that diverts the low-level easterly flows upward. Since simulated precipitation is weaker with ACM2, such upward diversion is less so that easterly

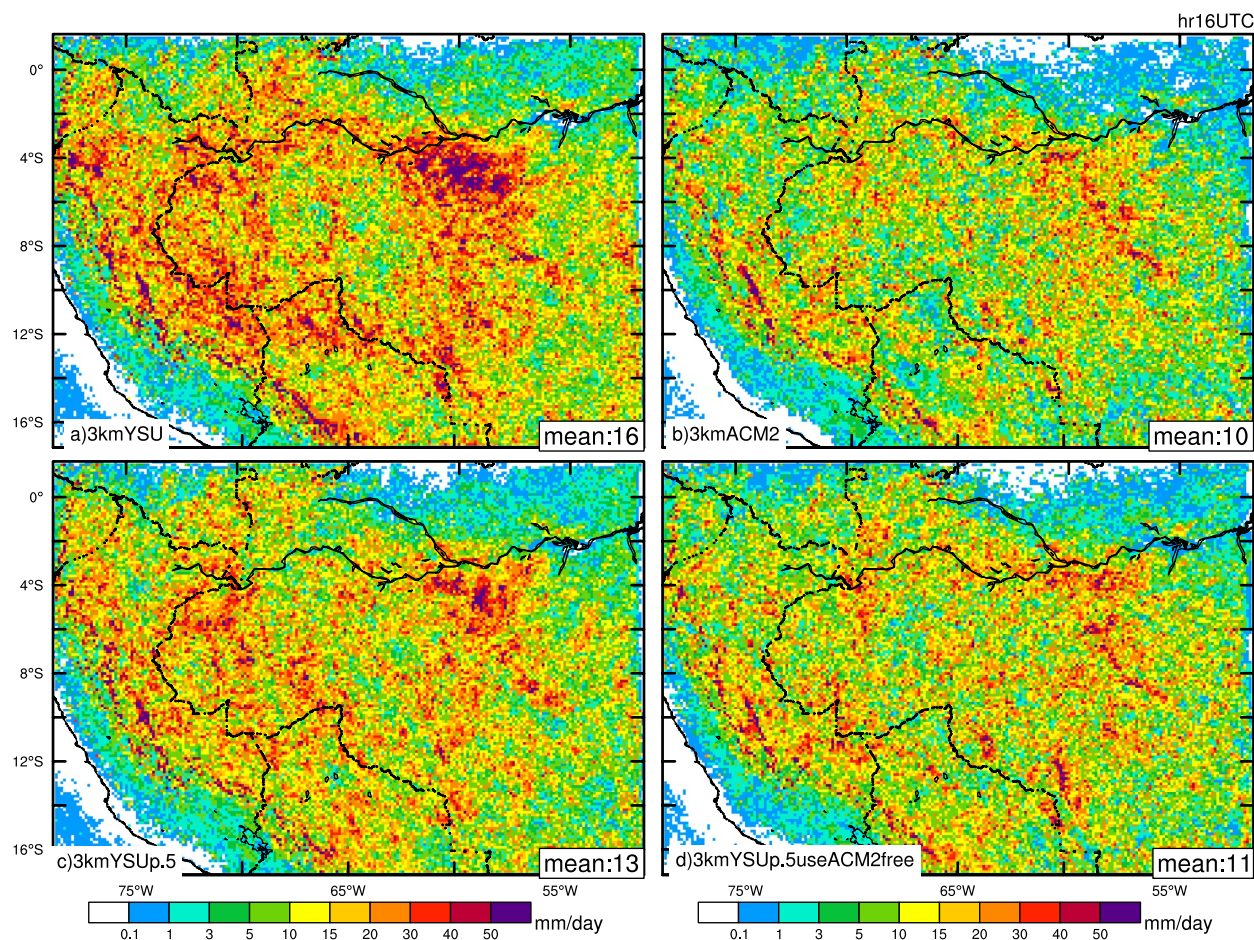


Figure 13. Average noon-time precipitation rate in January–February 2019 simulated by (a) 3kmYSU, (b) 3kmACM2, (c) 3kmYSUp.5, and (d) 3kmYSUp.5useACM2free. The domain-averaged values are marked.

winds leaving the Amazon and impinging on the east side of Andes are stronger, leading to stronger southward LLJ east of Andes when the easterly flows are diverted southward by the mountain range. While south American LLJ depends on the subtropical weather patterns, such as the Bolivia high, the Chaco low (Boers et al., 2015; Montini et al., 2019; Salio et al., 2002; Seiler et al., 2013; Vera, Baez, et al., 2006). It is modulated by the convection/turbulence interactions over the Amazon. Thus, the simulated strength of Amazonian precipitation is closely linked to the strength of LLJ east of Andes, which may have implications for the simulation of downstream atmospheric environments including temperature and humidity conditions and air quality (Hu, Klein, Xue, Lundquist, et al., 2013; Hu, Klein, Xue, Zhang, et al., 2013; Klein et al., 2014). These are topics for future studies.

Data Availability Statement

The ERA5 reanalysis data (Hersbach et al., 2020) are available at <https://doi.org/10.5065/BH6N-5N20>. GPM IMERG Final Precipitation data set is from Huffman et al. (2019). CMORPH data set (Joyce et al., 2004) is available at https://ftp.cpc.ncep.noaa.gov/precip/CMORPH_V1.0/CRT/8km-30min (last access: 12 November 2020). Figures in this manuscript are produced using the NCAR Command Language (Version 6.6.2) [Software] (2019). Model data produced from this study have been archived at CAPS website <https://caps.ou.edu/micronet/Regionalclimate.html> and the Luster NSF projects data server at the San Diego Super computer Center/expanse/luster/projects/uok114/xhu2.

Acknowledgments

This work was primarily supported by Grant 20163646499 from the Universidad Nacional de San Agustín de Arequipa (UNSA) of Peru through the IREES/LASI Global Change and Human Health Institute. The first author is partially supported by the National Mesonet Program Grant 10558200 and DOE ASR project (DE-SC0021159). Ming Xue was also supported by NSF Grant AGS-1917701. We are grateful to Bowen Zhou, Lan Gao and Jonathan E. Pleim for discussion. The simulations were performed on supercomputer Stampede 2 at the Texas Advanced Computing Center (TACC) through allocations TG-MCA95C006, and TG-ATM160014 from the Advanced Cyberinfrastructure Coordination Ecosystem: Services & Support (ACCESS) program, which is supported by National Science Foundation Grants 2138259, 2138286, 2138307, 2137603, and 2138296. The authors also acknowledge high-performance computing support from Cheyenne (<https://doi.org/10.5065/D6RX99HX>) provided by NCAR's Computational and Information Systems Laboratory. NCAR is sponsored by the National Science Foundation. Some of the post-processing of simulations for this work was performed at the University of Oklahoma (OU) Supercomputing Center for Education and Research (OSCR).

References

- Adebiyi, A. A., Zuidema, P., Chang, I., Burton, S. P., & Cairns, B. (2020). Mid-level clouds are frequent above the southeast Atlantic stratocumulus clouds. *Atmospheric Chemistry and Physics*, 20(18), 11025–11043. <https://doi.org/10.5194/acp-20-11025-2020>
- Adler, R. F., Gu, G., Sapiro, M., Wang, J.-J., & Huffman, G. J. (2017). Global precipitation: Means, variations and trends during the satellite era (1979–2014). *Surveys in Geophysics*, 38(4), 679–699. <https://doi.org/10.1007/s10712-017-9416-4>
- Angevine, W. M., Eddington, L., Durkee, K., Fairall, C., Bianco, L., & Brioude, J. (2012). Meteorological model evaluation for CalNex 2010. *Monthly Weather Review*, 140(12), 3885–3906. <https://doi.org/10.1175/Mwr-D-12-00042.1>
- Angevine, W. M., Jiang, H. L., & Mauritsen, T. (2010). Performance of an eddy diffusivity-mass flux scheme for shallow cumulus boundary layers. *Monthly Weather Review*, 138(7), 2895–2912. <https://doi.org/10.1175/2010mwr3142.1>
- Barber, K. A., Burleyson, C. D., Feng, Z., & Hagos, S. M. (2022). The influence of shallow cloud populations on transitions to deep convection in the Amazon. *Journal of the Atmospheric Sciences*, 79(3), 723–743. <https://doi.org/10.1175/jas-d-21-0141.1>
- Beare, R. J., MacVean, M. K., Holtslag, A. A. M., Cuxart, J., Esau, I., Golaz, J. C., et al. (2006). An intercomparison of large-eddy simulations of the stable boundary layer. *Boundary-Layer Meteorology*, 118(2), 247–272. <https://doi.org/10.1007/s10546-004-2820-6>
- Boers, N., Barbosa, H. M. J., Bookhagen, B., Marengo, J. A., Marwan, N., & Kurths, J. (2015). Propagation of strong rainfall events from southeastern South America to the central Andes. *Journal of Climate*, 28(19), 7641–7658. <https://doi.org/10.1175/JCLI-D-15-0137.1>
- Bright, D. R., & Mullen, S. L. (2002). The sensitivity of the numerical simulation of the southwest monsoon boundary layer to the choice of PBL turbulence parameterization in MM5. *Weather and Forecasting*, 17(1), 99–114. [https://doi.org/10.1175/1520-0434\(2002\)017<0099:Totsn>2.0.Co;2](https://doi.org/10.1175/1520-0434(2002)017<0099:Totsn>2.0.Co;2)
- Burleyson, C. D., & Yuter, S. E. (2015). Patterns of diurnal marine stratocumulus cloud fraction variability. *Journal of Applied Meteorology and Climatology*, 54(4), 847–866. <https://doi.org/10.1175/jamc-d-14-0178.1>
- Chakraborty, S., Jiang, J. H., Su, H., & Fu, R. (2020). Deep convective evolution from shallow clouds over the Amazon and Congo rainforests. *Journal of Geophysical Research: Atmospheres*, 125(1), e2019JD030962. <https://doi.org/10.1029/2019JD030962>
- Chakraborty, S., Schiro, K. A., Fu, R., & Neelin, J. D. (2018). On the role of aerosols, humidity, and vertical wind shear in the transition of shallow-to-deep convection at the Green Ocean Amazon 2014/5 site. *Atmospheric Chemistry and Physics*, 18(15), 11135–11148. <https://doi.org/10.5194/acp-18-11135-2018>
- Chen, F., & Zhang, Y. (2009). On the coupling strength between the land surface and the atmosphere: From viewpoint of surface exchange coefficients. *Geophysical Research Letters*, 36(10), L10404. <https://doi.org/10.1029/2009gl037980>
- Chen, M., Huang, Y., Li, Z., Larico, A. J. M., Xue, M., Hong, Y., et al. (2022). Cross-Examining precipitation products by rain gauge, remote sensing, and WRF simulations over a South American region across the Pacific coast and Andes. *Atmosphere*, 13(10), 1666. <https://doi.org/10.3390/atmos13101666>
- Clark, A. J., Coniglio, M. C., Coffey, B. E., Thompson, G., Xue, M., & Kong, F. Y. (2015). Sensitivity of 24-h forecast dryline position and structure to boundary layer parameterizations in convection-allowing WRF model simulations. *Weather and Forecasting*, 30(3), 613–638. <https://doi.org/10.1175/Waf-D-14-00078.1>
- Cohen, A. E., Cavallo, S. M., Coniglio, M. C., & Brooks, H. E. (2015). A review of planetary boundary layer parameterization schemes and their sensitivity in simulating southeastern US Cold season severe weather environments. *Weather and Forecasting*, 30(3), 591–612. <https://doi.org/10.1175/Waf-D-14-00105.1>
- Coniglio, M. C., Correia, J., Marsh, P. T., & Kong, F. Y. (2013). Verification of convection-allowing WRF model forecasts of the planetary boundary layer using sounding observations. *Weather and Forecasting*, 28(3), 842–862. <https://doi.org/10.1175/Waf-D-12-00103.1>
- Cuxart, J., Holtslag, A. A. M., Beare, R. J., Bazile, E., Beljaars, A., Cheng, A., et al. (2006). Single-column model intercomparison for a stably stratified atmospheric boundary layer. *Boundary-Layer Meteorology*, 118(2), 273–303. <https://doi.org/10.1007/s10546-005-3780-1>
- Durran, D. R., & Klemp, J. B. (1982). On the effects of moisture on the Turan-Väistälä frequency. *Journal of the Atmospheric Sciences*, 39(10), 2152–2158. [https://doi.org/10.1175/1520-0469\(1982\)039<2152:Oteomo>2.0.Co;2](https://doi.org/10.1175/1520-0469(1982)039<2152:Oteomo>2.0.Co;2)
- Fu, R., Zhu, B., & Dickinson, R. E. (1999). How do atmosphere and land surface influence seasonal changes of convection in the tropical Amazon? *Journal of Climate*, 12(5), 1306–1321. [https://doi.org/10.1175/1520-0442\(1999\)012<1306:Hdaals>2.0.Co;2](https://doi.org/10.1175/1520-0442(1999)012<1306:Hdaals>2.0.Co;2)
- Giangrande, S. E., Feng, Z., Jensen, M. P., Comstock, J. M., Johnson, K. L., Toto, T., et al. (2017). Cloud characteristics, thermodynamic controls and radiative impacts during the Observations and Modeling of the Green Ocean Amazon (GoAmazon2014/5) experiment. *Atmospheric Chemistry and Physics*, 17(23), 14519–14541. <https://doi.org/10.5194/acp-17-14519-2017>
- Giangrande, S. E., Wang, D., & Mecham, D. B. (2020). Cloud regimes over the Amazon Basin: Perspectives from the GoAmazon2014/5 campaign. *Atmospheric Chemistry and Physics*, 20(12), 7489–7507. <https://doi.org/10.5194/acp-20-7489-2020>
- Gopalakrishnan, D., Taraphdar, S., Pauluis, O. M., Xue, L., Ajayamohan, R. S., Al Shamsi, N., et al. (2023). Anatomy of a summertime convective event over the Arabian region. *Monthly Weather Review*, 151(4), 989–1004. <https://doi.org/10.1175/MWR-D-22-0082.1>
- Gunwani, P., & Mohan, M. (2017). Sensitivity of WRF model estimates to various PBL parameterizations in different climatic zones over India. *Atmospheric Research*, 194, 43–65. <https://doi.org/10.1016/j.atmosres.2017.04.026>
- Hersbach, H., Bell, B., Berrisford, P., Hirahara, S., Horányi, A., Muñoz-Sabater, J., et al. (2020). The ERA5 global reanalysis. *Quarterly Journal of the Royal Meteorological Society*, 146(730), 1999–2049. <https://doi.org/10.1002/qj.3803>
- Hong, S. Y. (2010). A new stable boundary-layer mixing scheme and its impact on the simulated East Asian summer monsoon. *Quarterly Journal of the Royal Meteorological Society*, 136(651), 1481–1496. <https://doi.org/10.1002/qj.665>
- Hong, S. Y., Noh, Y., & Dudhia, J. (2006). A new vertical diffusion package with an explicit treatment of entrainment processes. *Monthly Weather Review*, 134(9), 2318–2341. <https://doi.org/10.1175/Mwr3199.1>
- Hu, X.-M., Doughty, D. C., Sanchez, K. J., Joseph, E., & Fuentes, J. D. (2012). Ozone variability in the atmospheric boundary layer in Maryland and its implications for vertical transport model. *Atmospheric Environment*, 46, 354–364. <https://doi.org/10.1016/j.atmosenv.2011.09.054>
- Hu, X.-M., Klein, P. M., & Xue, M. (2013). Evaluation of the updated YSU planetary boundary layer scheme within WRF for wind resource and air quality assessments. *Journal of Geophysical Research-Atmospheres*, 118(18), 10490–10505. <https://doi.org/10.1002/jgrd.50823>
- Hu, X.-M., Klein, P. M., Xue, M., Lundquist, J. K., Zhang, F., & Qi, Y. (2013). Impact of low-level jets on the nocturnal urban heat island intensity in Oklahoma City. *Journal of Applied Meteorology and Climatology*, 52(8), 1779–1802. <https://doi.org/10.1175/jamc-d-12-0256.1>
- Hu, X.-M., Klein, P. M., Xue, M., Zhang, F., Doughty, D. C., Forkel, R., et al. (2013). Impact of the vertical mixing induced by low-level jets on boundary layer ozone concentration. *Atmospheric Environment*, 70, 123–130. <https://doi.org/10.1016/j.atmosenv.2012.12.046>
- Hu, X.-M., Nielsen-Gammon, J. W., & Zhang, F. Q. (2010). Evaluation of three planetary boundary layer schemes in the WRF model. *Journal of Applied Meteorology and Climatology*, 49(9), 1831–1844. <https://doi.org/10.1175/2010jamc2432.1>
- Hu, X.-M., Xue, M., & Li, X. (2019). The use of high-resolution sounding data to evaluate and optimize nonlocal PBL schemes for simulating the slightly stable upper convective boundary layer. *Monthly Weather Review*, 147(10), 3825–3841. <https://doi.org/10.1175/mwr-d-19-0085.1>

- Hu, X.-M., Xue, M., McPherson, R. A., Martin, E., Rosendahl, D. H., & Qiao, L. (2018). Precipitation dynamical downscaling over the Great Plains. *Journal of Advances in Modeling Earth Systems*, 10(2), 421–447. <https://doi.org/10.1002/2017ms001154>
- Hu, X.-M., Zhang, F., & Nielsen-Gammon, J. W. (2010). Ensemble-based simultaneous state and parameter estimation for treatment of mesoscale model error: A real-data study. *Geophysical Research Letters*, 37(8), L08802. <https://doi.org/10.1029/2010gl043017>
- Huang, H. Y., Hall, A., & Teixeira, J. (2013). Evaluation of the WRF PBL parameterizations for marine boundary layer clouds: Cumulus and stratocumulus. *Monthly Weather Review*, 141(7), 2265–2271. <https://doi.org/10.1175/Mwr-D-12-00292.1>
- Huang, Y., Xue, M., Hu, X.-M., Martin, E. R., Novoa, H., & McPherson, R. A. (2021). Convection-permitting regional climate simulations over South America and the Peruvian central Andes: Evaluation of precipitation and MCS simulations and sensitivity to physics parameterizations. Paper presented at the AGU Fall Meeting, New Orleans, LA. Retrieved from <https://agu2021fallmeeting.agu.ipostersessions.com/?s=A8-A3-C9-83-2A-48-C5-B0-72-9E-E3-46-AD-14-1A-7E>
- Huang, Y., Xue, M., Hu, X.-M., Martin, E. R., Novoa, H., McPherson, R. A., et al. (2023). Convection-permitting simulations of precipitation over the Peruvian Central Andes: Strong sensitivity to planetary boundary layer parameterization. *ESS Open Archive*. <https://doi.org/10.22541/essoar.168500290.09079234/v1>
- Huffman, G. J., Stocker, E. F., Bolvin, D. T., Nelkin, E. J., & Tan, J. (2019). GPM IMERG final precipitation L3 1 day 0.1 degree × 0.1 degree V06. <https://doi.org/10.5067/GPM/IMERGDF/DAY/06>
- Iacono, M. J., Delamere, J. S., Mlawer, E. J., Shephard, M. W., Clough, S. A., & Collins, W. D. (2008). Radiative forcing by long-lived greenhouse gases: Calculations with the AER radiative transfer models. *Journal of Geophysical Research*, 113(D13), D13103. <https://doi.org/10.1029/2008JD009944>
- Jankov, I., Gallus, W. A., Segal, M., Shaw, B., & Koch, S. E. (2005). The impact of different WRF model physical parameterizations and their interactions on warm season MCS rainfall. *Weather and Forecasting*, 20(6), 1048–1060. <https://doi.org/10.1175/Waf888.1>
- Jankov, I., Schultz, P. J., Anderson, C. J., & Koch, S. E. (2007). The impact of different physical parameterizations and their interactions on cold season QPF in the American River basin. *Journal of Hydrometeorology*, 8(5), 1141–1151. <https://doi.org/10.1175/jhm630.1>
- Jiménez, P. A., Dudhia, J., González-Rouco, J. F., Navarro, J., Montávez, J. P., & García-Bustamante, E. (2012). A revised scheme for the WRF surface layer formulation. *Monthly Weather Review*, 140(3), 898–918. <https://doi.org/10.1175/mwr-d-11-00056.1>
- Joyce, R. J., Janowiak, J. E., Arkin, P. A., & Xie, P. (2004). CMORPH: A method that produces global precipitation estimates from passive microwave and infrared data at high spatial and temporal resolution. *Journal of Hydrometeorology*, 5(3), 487–503. [https://doi.org/10.1175/1525-7541\(2004\)005<0487:Camtpg>2.0.co;2](https://doi.org/10.1175/1525-7541(2004)005<0487:Camtpg>2.0.co;2)
- Kay, J. E., Bourdages, L., Miller, N. B., Morrison, A., Yettella, V., Chepfer, H., & Eaton, B. (2016). Evaluating and improving cloud phase in the Community Atmosphere Model version 5 using spaceborne lidar observations. *Journal of Geophysical Research: Atmospheres*, 121(8), 4162–4176. <https://doi.org/10.1002/2015JD024699>
- Kay, J. E., Hillman, B. R., Klein, S. A., Zhang, Y., Medeiros, B., Pincus, R., et al. (2012). Exposing global cloud biases in the community atmosphere model (CAM) Using satellite observations and their corresponding instrument simulators. *Journal of Climate*, 25(15), 5190–5207. <https://doi.org/10.1175/jcli-d-11-00469.1>
- Klein, P. M., Hu, X.-M., & Xue, M. (2014). Impacts of mixing processes in nocturnal atmospheric boundary layer on urban ozone concentrations. *Boundary-Layer Meteorology*, 150(1), 107–130. <https://doi.org/10.1007/s10546-013-9864-4>
- Langenbrunner, B., Pritchard, M. S., Kooperman, G. J., & Randerson, J. T. (2019). Why does Amazon precipitation decrease when tropical forests respond to increasing CO₂? *Earth's Future*, 7(4), 450–468. <https://doi.org/10.1029/2018EF001026>
- Li, X. L., & Pu, Z. X. (2008). Sensitivity of numerical simulation of early rapid intensification of Hurricane Emily (2005) to cloud microphysical and planetary boundary layer parameterizations. *Monthly Weather Review*, 136(12), 4819–4838. <https://doi.org/10.1175/2008mwr2366.1>
- Lilly, D. K. (1968). Models of cloud-topped mixed layers under a strong inversion. *Quarterly Journal of the Royal Meteorological Society*, 94(401), 292–309. <https://doi.org/10.1002/qj.49709440106>
- Liu, C., Ikeda, K., Rasmussen, R., Dominguez, F., Prein, A. F., Dudhia, J., & Chen, F. (2022). An overview of two-decade-long convection permitting regional climate downscaling over the continental South America. Paper presented at the AGU fall meeting, Chicago, IL. Retrieved from <https://agu.confex.com/agu/fm22/meetingapp.cgi/Paper/1115319>
- Liu, M., & Carroll, J. J. (1996). A high-resolution air pollution model suitable for dispersion studies in complex terrain. *Monthly Weather Review*, 124(10), 2396–2409. [https://doi.org/10.1175/1520-0493\(1996\)124<2396:Ahrpm>2.0.co;2](https://doi.org/10.1175/1520-0493(1996)124<2396:Ahrpm>2.0.co;2)
- Lu, X., & Wang, X. (2019). Improving hurricane analyses and predictions with TCI, IFEX field campaign observations, and CIMSS AMVs using the advanced hybrid data assimilation system for HWRF. Part I: What is missing to capture the rapid intensification of Hurricane Patricia (2015) when HWRF is already initialized with a more realistic analysis? *Monthly Weather Review*, 147(4), 1351–1373. <https://doi.org/10.1175/mwr-d-18-0202.1>
- Miguez-Macho, G., Stenchikov, G. L., & Robock, A. (2004). Spectral nudging to eliminate the effects of domain position and geometry in regional climate model simulations. *Journal of Geophysical Research*, 109(D13), D13104. <https://doi.org/10.1029/2003jd004495>
- Miguez-Macho, G., Stenchikov, G. L., & Robock, A. (2005). Regional climate simulations over North America: Interaction of local processes with improved large-scale flow. *Journal of Climate*, 18(8), 1227–1246. <https://doi.org/10.1175/Jcli3369.1>
- Montini, T. L., Jones, C., & Carvalho, L. M. V. (2019). The South American low-level jet: A new climatology, variability, and changes. *Journal of Geophysical Research: Atmospheres*, 124(3), 1200–1218. <https://doi.org/10.1029/2018JD029634>
- Nakanishi, M., & Niino, H. (2006). An improved Mellor–Yamada level-3 model: Its numerical stability and application to a regional prediction of advection fog. *Boundary-Layer Meteorology*, 119(2), 397–407. <https://doi.org/10.1007/s10546-005-9030-8>
- NCAR Command Language. (2019). NCAR Command Language (version 6.6.2) [Software]. UCAR/NCAR/CISL/TDD. <https://doi.org/10.5065/D6WD3XH5>
- Nielsen-Gammon, J. W., Hu, X.-M., Zhang, F., & Pleim, J. E. (2010). Evaluation of planetary boundary layer scheme sensitivities for the purpose of parameter estimation. *Monthly Weather Review*, 138(9), 3400–3417. <https://doi.org/10.1175/2010mwr3292.1>
- Noh, Y., Cheon, W. G., Hong, S. Y., & Raasch, S. (2003). Improvement of the K-profile model for the planetary boundary layer based on large eddy simulation data. *Boundary-Layer Meteorology*, 107(2), 401–427. <https://doi.org/10.1023/A:1022146015946>
- Olson, J. B., Kenyon, J. S., Angevine, W. A., Brown, J. M., Pagowski, M., & Sušelj, K. (2019). A description of the MYNN-EDMF scheme and the coupling to other components in WRF-ARW. <https://doi.org/10.25923/n9wm-be49>
- Olson, J. B., Kenyon, J. S., Djalalova, I., Bianco, L., Turner, D. D., Pichugina, Y., et al. (2019). Improving wind energy forecasting through numerical weather prediction model development. *Bulletin of the American Meteorological Society*, 100(11), 2201–2220. <https://doi.org/10.1175/bams-d-18-0040.1>

- Painemal, D., Xu, K.-M., Cheng, A., Minnis, P., & Palikonda, R. (2015). Mean structure and diurnal cycle of southeast Atlantic boundary layer clouds: Insights from satellite observations and multiscale modeling framework simulations. *Journal of Climate*, 28(1), 324–341. <https://doi.org/10.1175/jcli-d-14-00368.1>
- Pergaud, J., Masson, V., Malarde, S., & Couvreux, F. (2009). A parameterization of dry thermals and shallow cumuli for mesoscale numerical weather prediction. *Boundary-Layer Meteorology*, 132(1), 83–106. <https://doi.org/10.1007/s10546-009-9388-0>
- Pleim, J. E. (2007a). A combined local and nonlocal closure model for the atmospheric boundary layer. Part I: Model description and testing. *Journal of Applied Meteorology and Climatology*, 46(9), 1383–1395. <https://doi.org/10.1175/Jam2539.1>
- Pleim, J. E. (2007b). A combined local and nonlocal closure model for the atmospheric boundary layer. Part II: Application and evaluation in a mesoscale meteorological model. *Journal of Applied Meteorology and Climatology*, 46(9), 1396–1409. <https://doi.org/10.1175/Jam2534.1>
- Prein, A. F., Ge, M., Valle, A. R., Wang, D., & Giangrande, S. E. (2022). Towards a unified setup to simulate mid-latitude and tropical mesoscale convective systems at kilometer-scales. *Earth and Space Science*, 9(8), e2022EA002295. <https://doi.org/10.1029/2022EA002295>
- Prein, A. F., Langhans, W., Fosser, G., Ferrone, A., Ban, N., Goergen, K., et al. (2015). A review on regional convection-permitting climate modeling: Demonstrations, prospects, and challenges. *Reviews of Geophysics*, 53(2), 323–361. <https://doi.org/10.1002/2014rg000475>
- Prein, A. F., Rasmussen, R. M., Ikeda, K., Liu, C., Clark, M. P., & Holland, G. J. (2017). The future intensification of hourly precipitation extremes. *Nature Climate Change*, 7(1), 48–52. <https://doi.org/10.1038/nclimate3168>
- Salio, P., Nicolini, M., & Saulo, A. C. (2002). Chaco low-level jet events characterization during the austral summer season. *Journal of Geophysical Research*, 107(D24), ACL 32–31–ACL 32–17. <https://doi.org/10.1029/2001JD001315>
- Seiler, C., Hutjes, R. W. A., & Kabat, P. (2013). Climate variability and trends in Bolivia. *Journal of Applied Meteorology and Climatology*, 52(1), 130–146. <https://doi.org/10.1175/JAMC-D-12-0105.1>
- Shin, H. H., & Hong, S. Y. (2011). Intercomparison of planetary boundary-layer parametrizations in the WRF model for a single day from CASES-99. *Boundary-Layer Meteorology*, 139(2), 261–281. <https://doi.org/10.1007/s10546-010-9583-z>
- Skamarock, W. C., & Klemp, J. B. (2008). A time-split nonhydrostatic atmospheric model for weather research and forecasting applications. *Journal of Computational Physics*, 227(7), 3465–3485. <https://doi.org/10.1016/j.jcp.2007.01.037>
- Skamarock, W. C., Klemp, J. B., Dudhia, J., Gill, D. O., Liu, Z., Berner, J., et al. (2021). A description of the advanced research WRF model Version 4.3. (NCAR/TN-556+STR). <https://doi.org/10.5065/df8-6p97>
- Sun, X. G., Xue, M., Brotzge, J., McPherson, R. A., Hu, X.-M., & Yang, X. Q. (2016). An evaluation of dynamical downscaling of Central Plains summer precipitation using a WRF-based regional climate model at a convection-permitting 4 km resolution. *Journal of Geophysical Research-Atmospheres*, 121(23), 13801–13825. <https://doi.org/10.1002/2016jd024796>
- Supinie, T. A., Park, J., Snook, N., Hu, X.-M., Brewster, K. A., Xue, M., & Carley, J. R. (2022). Cool-season evaluation of FV3-LAM-based CONUS-scale forecasts with physics configurations of experimental RRFS ensembles. *Monthly Weather Review*, 150(9), 2379–2398. <https://doi.org/10.1175/mwr-d-21-0331.1>
- Tai, S.-L., Feng, Z., Ma, P.-L., Schumacher, C., & Fast, J. D. (2021). Representations of precipitation diurnal cycle in the Amazon as simulated by observationally constrained cloud-system resolving and global climate models. *Journal of Advances in Modeling Earth Systems*, 13(11), e2021MS002586. <https://doi.org/10.1029/2021MS002586>
- Thompson, G., Field, P. R., Rasmussen, R. M., & Hall, W. D. (2008). Explicit forecasts of winter precipitation using an improved bulk micro-physics scheme. Part II: Implementation of a new snow parameterization. *Monthly Weather Review*, 136(12), 5095–5115. <https://doi.org/10.1175/2008mwr2387.1>
- Tiedtke, M. (1989). A comprehensive mass flux scheme for cumulus parameterization in large-scale models. *Monthly Weather Review*, 117(8), 1779–1800. [https://doi.org/10.1175/1520-0493\(1989\)117<1779:Acmsf>2.0.Co;2](https://doi.org/10.1175/1520-0493(1989)117<1779:Acmsf>2.0.Co;2)
- Troen, I., & Mahrt, L. (1986). A simple-model of the atmospheric boundary-layer—Sensitivity to surface evaporation. *Boundary-Layer Meteorology*, 37(1–2), 129–148. <https://doi.org/10.1007/BF00122760>
- Valappil, V. K., Kedia, S., Dwivedi, A. K., Pokale, S. S., Islam, S., & Khare, M. K. (2023). Assessing the performance of WRF ARW model in simulating heavy rainfall events over the Pune region: In support of operational applications. *Meteorology and Atmospheric Physics*, 135(2), 16. <https://doi.org/10.1007/s00703-023-00952-7>
- Vera, C., Baez, J., Douglas, M., Emmanuel, C. B., Marengo, J., Meitin, J., et al. (2006). The South American low-level jet experiment. *Bulletin of the American Meteorological Society*, 87(1), 63–78. <https://doi.org/10.1175/BAMS-87-1-63>
- Vera, C., Silvestri, G., Liebmann, B., & González, P. (2006). Climate change scenarios for seasonal precipitation in South America from IPCC-AR4 models. *Geophysical Research Letters*, 33(13), L13707. <https://doi.org/10.1029/2006GL025759>
- Vilà-Guerau de Arellano, J., Wang, X., Pedruzo-Bagazgoitia, X., Sikma, M., Agustí-Panareda, A., Boussetta, S., et al. (2020). Interactions between the amazonian rainforest and cumuli clouds: A large-eddy simulation, high-resolution ECMWF, and observational intercomparison study. *Journal of Advances in Modeling Earth Systems*, 12(7), e2019MS001828. <https://doi.org/10.1029/2019MS001828>
- Wang, J. L., & Kotamarthi, V. R. (2013). Assessment of dynamical downscaling in near-surface fields with different spectral nudging approaches using the nested regional climate model (NRCM). *Journal of Applied Meteorology and Climatology*, 52(7), 1576–1591. <https://doi.org/10.1175/Jamc-D-12-0302.1>
- Wang, J. X., & Hu, X.-M. (2021). Evaluating the performance of WRF urban schemes and PBL schemes over Dallas-Fort Worth during a dry summer and a wet summer. *Journal of Applied Meteorology and Climatology*, 60(6), 779–798. <https://doi.org/10.1175/Jamc-D-19-0195.1>
- Wang, W. G., Shen, X. Y., & Huang, W. Y. (2016). A comparison of boundary-layer characteristics simulated using different parametrization schemes. *Boundary-Layer Meteorology*, 161(2), 375–403. <https://doi.org/10.1007/s10546-016-0175-4>
- Wright, J. S., Fu, R., Worden, J. R., Chakraborty, S., Clinton, N. E., Risi, C., et al. (2017). Rainforest-initiated wet season onset over the southern Amazon. *Proceedings of the National Academy of Sciences*, 114(32), 8481–8486. <https://doi.org/10.1073/pnas.1621516114>
- Wu, M., Lee, J.-E., Wang, D., & Salameh, M. (2021). Suppressed daytime convection over the Amazon River. *Journal of Geophysical Research: Atmospheres*, 126(13), e2020JD033627. <https://doi.org/10.1029/2020JD033627>
- Wu, Z., Li, Y., Li, X., Hu, X.-M., Zhou, G., & Deng, C. (2021). Influence of different planetary boundary layer parameterization schemes on the simulation of precipitation caused by southwest China vortex in Sichuan basin based on the WRF model. *Chinese Journal of Atmospheric Sciences*, 45(1), 58. <https://doi.org/10.3878/j.issn.1006-9895.2005.19171>
- Xie, B., Fung, J. C. H., Chan, A., & Lau, A. (2012). Evaluation of nonlocal and local planetary boundary layer schemes in the WRF model. *Journal of Geophysical Research*, 117(D12). <https://doi.org/10.1029/2011JD017080>
- Yang, Y., Hu, X.-M., Gao, S., & Wang, Y. (2019). Sensitivity of WRF simulations with the YSU PBL scheme to the lowest model level height for a sea fog event over the Yellow Sea. *Atmospheric Research*, 215, 253–267. <https://doi.org/10.1016/j.atmosres.2018.09.004>
- Zhang, D., Wang, Z., & Liu, D. (2010). A global view of midlevel liquid-layer topped stratiform cloud distribution and phase partition from CALIPSO and CloudSat measurements. *Journal of Geophysical Research*, 115(D4), D00H13. <https://doi.org/10.1029/2009JD012143>

- Zhang, Y., Jiang, Y., & Tan, B. (2013). Influences of different PBL schemes on secondary eyewall formation and eyewall replacement cycle in simulated Typhoon Sinlaku (2008). *Acta Meteorologica Sinica*, 27(3), 322–334. <https://doi.org/10.1007/s13351-013-0312-7>
- Zhu, P., Hazelton, A., Zhang, Z., Marks, F. D., & Tallapragada, V. (2021). The role of eyewall turbulent transport in the pathway to intensification of tropical cyclones. *Journal of Geophysical Research: Atmospheres*, 126(17), e2021JD034983. <https://doi.org/10.1029/2021JD034983>
- Zhu, P., Tyner, B., Zhang, J. A., Aligo, E., Gopalakrishnan, S., Marks, F. D., et al. (2019). Role of eyewall and rainband eddy forcing in tropical cyclone intensification. *Atmospheric Chemistry and Physics*, 19(22), 14289–14310. <https://doi.org/10.5194/acp-19-14289-2019>